GENETIC DISSECTION OF MURINE LUPUS SUSCEPTIBILITY LOCUS *SLE1C* IDENTIFIES ESTROGEN-RELATED RECEPTOR GAMMA AS A NOVEL REGULATOR OF AUTOIMMUNITY

By

DANIEL JAMES PERRY

A DISSERTATION PRESENTED TO THE GRADUATE SCHOOL
OF THE UNIVERSITY OF FLORIDA IN PARTIAL FULFILLMENT
OF THE REQUIREMENTS FOR THE DEGREE OF
DOCTOR OF PHILOSOPHY

UNIVERSITY OF FLORIDA

2011

To my loving wife who supports me through thick and thin. Also to my mother who put herself through school while raising two children on her own. Their dedication is my inspiration.

ACKNOWLEDGMENTS

Much of the work in this project could not be done without the generous gift of FoxP3-eGFP knock in mice for Dr. Vijay Kuchroo at Harvard Medical School and the analysis of microarray data by Dr. Igor Dozmorov at Oklahoma Medical Research Center. I would also like to thank Neal Benson for his assistance with FACS sorting and Leilani Zeumer, Xuekun Su, and Jessica Lohmann for their excellent animal husbandry work. Also, several senior colleagues, including Kim Blenman, Biyan Duan, Zhiwei Xu, Carla Cuda, and Surya Potula were instrumental for technical assistance in almost every aspect of this project. I thank my committee for their critical advice and suggestions. Last but not least, I thank my mentor for the opportunity and continued guidance.

TABLE OF CONTENTS

page

LIST OF TABLES

LIST OF FIGURES

Abstract of Dissertation Presented to the Graduate School
of the University of Florida in Partial Fulfillment of the
Requirements for the Degree of Doctor of Philosophy

GENETIC DISSECTION OF MURINE LUPUS SUSCEPTIBILITY LOCUS *SLE1C* IDENTIFIES ESTROGEN-RELATED RECEPTOR GAMMA AS A NOVEL REGULATOR OF AUTOIMMUNITY

By

Daniel James Perry

August 2011

Chair: Laurence Marguerite Morel
Major: Medical Sciences – Immunology and Microbiology

Systemic lupus erythematosus (SLE) is a chronic autoinflammatory disease that manifests in many forms ranging from mild to acute and affecting multiple organ systems. It is characterized by the presence of pathogenic antinuclear antibodies (ANA) that result in the deposition of immune complexes in basement membranes throughout the body. These immune complexes can then induce inflammatory responses that over time lead to tissue destruction. This capability of tissue destruction anywhere in the body is the reason for the multifaceted nature of the disease. Patients with the highest mortality are those in which the kidneys are involved. In such cases, immune complex deposits result in glomerulonephritis (GN), eventually leading to kidney failure and death. Because the genetic and environmental factors that cause SLE are poorly understood, treatment is generally limited to regimens of immunosuppressive therapies, which tend to have detrimental side effects. Thus there is an imminent need for the discovery of improved treatments.

The focus of the work in our lab is on identifying genetic factors responsible for SLE etiology using the NZM2410 recombinant inbred mouse strain. Derived from NZB

and NZW, its parental strains are the basis of the classic NZB/W F1 lupus mouse model. Linkage analysis of a cohort of NZM x B6 F1 backcrossed to NZM identified three major lupus susceptibility loci. Among these, *Sle1*, located on Chromosome 1, has been shown to be required for initiation of the disease by mediating a loss of tolerance to nuclear antigens. Subsequently, *Sle1* was determined to be composed of three subloci, *Sle1a*, *Sle1b*, and *Sle1c*. Further characterization of the *Sle1c* sublocus found it to be a complex locus as well, with decreased germinal center and T dependent immune responses mapping to the telomeric portion, and $CD4^+$ T cell hyperactivation and increased chronic graft-versus-host disease (cGVHD) mapping to the centromeric portion of the locus. In this project phenotypic mapping was used to refine the centromeric *Sle1c2* sublocus to a 675Kb interval. Recombinant congenic strains with the NZW-derived *Sle1c2* interval introgressed exhibited $CD4^+$ T cell activation and cGVHD susceptibility, similar to mice with the parental *Sle1c*. In addition, B6.*Sle1c2* mice were found to have a robust expansion of INFγ expressing T_H1 cells. Also, when the *Sle1c2* locus in NZB x B6 F1 mice was NZB/NZW as compared to NZB/B6, B cell activation, autoantibody production, and GN were exacerbated, verifying the locus as a bona fide lupus susceptibility locus.

Of the two genes in the *Sle1c2* interval, only one, Estrogen-related receptor gamma (*Esrrg*), had detectable expression in $CD4^+$ T cells. Furthermore, congenic B6.*Sle1c2* mice expressed less *Esrrg* than B6 controls in $CD4^+$ T cells, and *Esrrg* expression had a very strong negative correlation to $CD4^+$ T cell activation. Taken together, I propose *Esrrg* to be a novel target for the therapeutic intervention of SLE.

CHAPTER 1
BACKGROUND AND RELEVENCE

Systemic Lupus Erythematosus

According to the CDC, the incidence of Systemic Lupus Erythematosus (SLE) is estimated to be between 300,000 and 4 million cases in the U.S. (1). SLE is an autoimmune disorder mediated by pathogenic immune attack on nuclear antigens, resulting in the production of anti-nuclear autoantibodies (ANA) whose specificities include double-stranded DNA (dsDNA), histones, chromatin/subnucleosome complexes, and ribonucleoproteins. High levels of these autoantibodies result in immune complex formation that is subsequently deposited in the basement membranes of various tissues. There, they induce inflammation and tissue destruction. Therefore, SLE has the ability to affect almost any organ system resulting in neurological, musculoskeletal, gastrointestinal, renal, cardiac, and pulmonary manifestations, as well as fever, fatigue, and malaise (2). Because of this heterogeneity of clinical symptoms, which tend to fluctuate with disease flares-up and remissions, diagnosis is never straightforward. Usually, SLE can be diagnosed if a patient exhibits at least four of the criteria on the American College of Rheumatology Revised Criteria for Classification of Systemic Lupus Erythematosus (Table 1-1) either serially or simultaneously (3, 4). This list of criteria does have several limitations, especially with diagnosing the onset of SLE, and revision efforts are in progress (5).

There is no cure for SLE, and currently, treatment is directed toward decreasing the frequency and severity of flares. This is largely achieved via a regimen of antimalarial, immunosuppressive, and anti-inflammatory treatments that tend to have serious side effects (6). Type I interferon is a major accelerator of disease flare-ups (7).

Hydroxychloroquine is an antimalarial that inhibits phagosome function, thereby attenuating toll-like receptor mediated type I interferon production. Glucocorticoids decrease B and T cell activation and usually require significant dose increases during flare-ups, which produce detrimental side effects. Cyclophosphamide is a chemotherapeutic that when metabolized by lymphocytes, cross-links DNA resulting in apoptosis. Azathioprine and mycophenolate mofetil both interfere with purine synthesis in lymphocytes, thereby inhibiting proliferation. There is also strong evidence for a number of biological therapies, however, the majority have failed clinical trials, with several more likely due to trial design than actual ineffectiveness (6). Still one, Belimumab, was reported to be effective and well tolerated in phase II and III clinical trials, and it became the first biological therapy approved by the FDA for treatment of active SLE in March of 2011 (8, 9). Belimumab is a human monoclonal antibody that binds and inhibits B-lymphocyte stimulator (BLyS; also known as BAFF), an important survival factor for B cells. The use of more effective biological therapies is expected to decrease the reliance on glucocorticoid and chemotherapeutic agents, thus reducing side effects, decreasing the frequency and severity of flare-ups, and improving quality of life for SLE patients.

Genetics of SLE in Humans

SLE is a complex genetic disorder, resulting from a combination of genetic and environmental factors that individually do not cause disease. The most compelling evidence of a genetic contribution in human SLE lies in the fact that incidence between monozygotic twins is roughly tenfold higher than in dizygotic twins and other full siblings (10, 11). In addition, there are strong familial association and race effects that dictate prevalence, age of onset, and severity (12-14).

Although it can affect males and females of any age, SLE onset most commonly occurs in women of child-bearing age. Thus, SLE exhibits a sexual dimorphism, common to many autoimmune diseases, such that nine females are affected for every one male. As this skewing suggests, there are clear effects of sex hormones and SLE onset and severity (15, 16). Additionally, murine models have shown a direct effect of estrogen both through castration/replenishment studies and through receptor knockout studies (17, 18). Also as expected, this gender difference is likely due to a dose effect of the X Chromosome, as men with Klinefelter Syndrome (47,XXY) have a similar prevalence of SLE as 46,XX women and about 14 fold higher prevalence as in 46,XY men (19).

The sex chromosome controlled hormones are not the whole story of the X Chromosomethat encodes a plethora of genes with immune function. Toll-like receptor 7 (*TLR7*) has been proven to be associated with disease pathogenesis. The second copy of *Tlr7* in a duplication translocation of part of the X Chromosome onto the Y Chromosome was discovered as the main functional contributor to the Y-linked autoimmune acceleration (*Yaa*) phenotype observed in mice (20-24). Subsequently, a study in humans found an allele of *TLR7* with associated risk for SLE development in males. Undoubtedly, such studies will find more of SLE associations of X-linked genes. Regardless, the fact that males are also susceptible is shows that autosomal genes also contribute to pathogenesis.

One way to identify genes responsible for SLE is through genetic association studies. These studies attempt to establish a relationship between the alleles at a given locus with disease by establishing that the frequency of a given allele within an affected

population is significantly higher than the overall population. The recent annotation of millions of single nucleotide polymorphisms (SNPs) in the human genome and the inception of high-throughput genotyping technologies has enabled the use of genome-wide association studies (GWAS) to simultaneously search entire genomes of large cohorts for causative alleles. To date, SLE susceptibility has been associated to dozens of genes by GWAS (25, 26). While these associations offer important new insights into SLE etiology, there are logistical limitations to GWAS. Extremely large sample sets are required to achieve significant associations and extrinsic factors such as ethnicity, clinical history, and lifestyle must be considered in choosing these sets. Further, GWAS are capable of identifying genomic associations but do not characterize the function that an allelic variation confers. For this, other methods are required.

Genetics of Lupus in Mice

In inbred strains of mice, it is possible to test whether a disease phenotype is linked to specific regions of the genome. To identify susceptibility loci, known as quantitative trait loci (QTL), susceptible strains are bred to resistant strains. A large cohort of N2 (F1 backcrossed to one of the parental strains) mice is then generated for phenotypic and genetic analysis. A genome-wide scan is conducted on all N2 mice using microsatellite markers that are polymorphic between the two parental strains. All mice are then assayed for selected phenotypes that are representative for the disease being studied and statistics are used to identify linkage between genetic regions and the selected phenotypes. Linkage analyses have already led to the discovery of roughly 3,000 mouse QTL for various diseases (27).

Congenic Dissection

Congenic dissection is an effective method to study the genetic factors that convey lupus susceptibility in the mouse because it offers the potential to study each locus, or identified susceptibility allele of a gene, individually and within a controlled genetic background. It involves the generation of recombinant congenic strains in which individual QTLs from susceptible strains are substituted onto the genome of a resistant strain (alternatively, resistance loci can be substituted onto the susceptible background). This relies on a marker-assisted selection breeding protocol to reduce the number of generations it takes to remove contaminating donor genome from the unlinked regions (28). This approach has proven successful in identifying genes responsible for other complex phenotypes, such as: differential isoform expression of *Ly108* has been shown to contribute to the NZM2410-derived lupus susceptibility locus, *Sle1b* (29, 30); a complex rearrangement in the promoter region of *Vnn3* has been shown to contribute to the A/J-derived malaria susceptibility locus, *Char9* (31); and a mutation of *Slc11a1* has been shown to result in the type 1 diabetes resistance of the B10-derived *Idd5.2* locus (32).

A common feature of linkage analyses is that they tend to identify QTLs that contain multiple physically linked genetic effects (27). To better define the location of the susceptibility allele(s) within the locus, genetic mapping is performed using subcongenic strains that are screened for the phenotypes associated with the locus. At this point, if the locus-associated phenotype has broken down and maps to multiple loci, subsequent rounds of genetic mapping may be necessary. If, however, the susceptibility locus maps to one sufficiently small genetic interval in which there are few (ideally one) genes, a complete functional characterization of the locus and genetic

analyses of potential candidate genes can be performed. Optimal identification of the susceptibility allele would involve the discovery of genetic polymorphisms that result in variances in expression or function of the gene product. Definitive proof would require that the associated phenotype be reconstituted when the susceptibility allele is expressed on the resistant parental genome.

Ultimately, animal models are employed to assist in studying human disorders. In this way, a collaborative approach should be used where linkage analysis and congenic dissection methods in murine models leads to the identification of candidate genes that should then be confirmed to be associated with human disease (if they aren't already). Murine models are also useful for candidate gene functional studies and drug testing before novel therapies can be tested in clinical trials (Figure 1-1).

The NZM2410 Model of Murine Lupus

The NZM2410 (NZM) mouse strain was derived from a (NZB x NZW) F1 x NZW backcross followed by inbreeding to homozygosity (33). It was found to replicate the spontaneous lupus like disease with increased severity and without the sexual dimorphism observed in the parental NZB/W F1 strain. An analysis of a cohort of NZM x B6 F1 backcrossed to NZM identified an association between GN and three loci on Chromosomes 1, 3, and 7, which were then termed *Sle1*, *Sle2*, and *Sle3* respectively (34). Recombinant congenic strains revealed that though these loci were implicated in the autoimmune phenotypes, each individual locus was not sufficient to initiate the fulminate disease seen in the parent NZM strain (35). This is characteristic of complex genetic disorders such that the genetic factors contributing to SLE susceptibility do not individually cause disease, but instead require epistatic interactions for pathogenesis.

Proof of this model came in the form of the B6.*Sle1/2/3* triple congenic strain, which reconstituted disease to a similar extent as that observed in the parental NZM strain (36).

Phenotypic characterization revealed that *Sle2* was associated with B cell hyperactivity and expansion of the B1a cell compartment (37). Recently, cyclin-dependent kinase inhibitor 2C (*Cdkn2c)* was identified as the candidate gene for *Sle2c1*, a sublocus of *Sle2* (38). A promoter polymorphism the in *Cdkn2c* was shown to result in decreased expression and consequent defective G1 arrest in B6.*Sle2c1* splenic B cells and peritoneal cavity B1a cells. This results in expansion of B1a cells and aberrant differentiation of splenic B cells into plasma cells.

Sle3 was initially associated with increased polyclonal and anti-nuclear antibody production as well as GN susceptibility (35). This locus was later found to consist of two loci, *Sle3* and *Sle5*, that were each capable of causing disease when combined with *Sle1* (39, 40). The increased GN severity caused by *Sle3* was found to be attributable to a cluster of kallikrein genes that can regulate the development of anti-glomerular basement membrane autoantibodies and have been associated with both SLE and spontaneous lupus nephritis in humans (41, 42).

Sle1 had the strongest linkage and was characterized by loss of tolerance to nuclear antigen and B and T cell hyperactivation (35, 43). Importantly, *Sle1* was found to be syntenic to the human SLE QTL 1q22-24 and 1q41-44 (44, 45). Also, it overlaps with SLE susceptibility loci from other mouse strains. These include *Cgnz1* from NZM2328, *Nba2* from NZB, and *Bxs3* from Bxsb.*Yaa* (46-49). Genetic mapping of *Sle1*

subsequently revealed the presence of multiple susceptibility loci, which were termed *Sle1a*, *Sle1b*, and *Sle1c* (50).

Sle1c is an ~7.5Mb NZW-derived locus, beginning somewhere in the centromeric recombination interval between *D1MIT459* and *D1MIT274* and extending to the telomere of Chromosome 1 (Figure 1-2). Importantly, *Sle1c* has been shown to accelerate autoimmunity in NZB x B6.*Sle1c* F1 mice, validating it as a lupus susceptibility locus (51). Two loci appear to be contributing to the overall *Sle1c* phenotype. This had been determined through B6.*Sle1c* subcongenic lines of mice that have since been discontinued. The first locus, *Sle1c1*, is telomeric to *D1MIT274*. Its phenotypes include decreased humoral response to T-dependent antigen and impaired germinal center (GC) formation and function (52). Evidence suggests a role for complement receptor 2 (*Cr2)* and not complement receptor related protein (Crry, *Cr1l*) that is only 5.2Kb from *Cr2* (53, 54). The NZW allele of *Cr2* exhibits reduced binding of its C3d ligand and reduces signaling that is predicted to be due to a non-synonymous coding SNP, predicted to introduce a novel glycosylation site and inhibit receptor dimerization. The second locus, *Sle1c2*, is centromeric to *D1MIT17* and is associated with T cell hyperactivation and proliferation, enhanced chronic graft-versus-host disease, and decreased T_{reg} numbers (52). The next chapter details my further refinement of the *Sle1c2* locus. The positional candidate genes centromeric to *D1MIT17* have not been described as having roles in the immune system. Since *Sle1c* is syntenic to human Chromosome 1q31-32, which has been linked to SLE (55), elucidation of the genetic factors responsible for *Sle1c2* is likely to reveal novel pathways that may be utilized for improved therapies for human autoimmunity.

Role of $CD4^+$ T cells in SLE

It has been 25 years since the initial classification of the T_H1 and T_H2 subsets CD4+ T cell subsets (56). Since then, several other subsets have been defined, most notably, T_{reg} and T_H17 cells. As will be discussed in the next chapter, *Sle1c2* confers T_H1 skewing and a T_H17 gene expression profile in congenic mice. In this section, these four subsets will be briefly described, followed by a detailed discussion of the roles of T_H1 and T_H17 cells in SLE pathogenesis.

$CD4^+$ T cells are classified into functional lineages based on the cytokines they produce. This is largely dictated by the circumstances in which they were activated as naïve cells. T cells require 3 signals from antigen presenting cells (APCs) for activation. For $CD4^+$ T cells, signal 1 is comprised of cognate peptide/major histocompatibility complex II (pMHCII) engagement of T cell receptors (TCRs). Signal 2 is sent through costimulatory surface molecules, most notably, B7 molecules on APCs interacting with CD28 on T cells. Finally, signal 3 is received from soluble cytokine molecules both from the milieu in which activation is occurring and directly from the activating APC at the immune synapse. It is this last signal that determines the fate of the naïve T cell.

The main induction cytokines for T_H1 cells are IL-12 and IL-18 (57). Receptor signaling is mediated by signal transducer and activator of transcription 4 (STAT4) and IL-1 receptor-associated kinase pathway, respectively. The net result of this signaling in combination with TCR and coreceptor signaling is activation of the T_H1 master transcription factor, T-box expressed in T cell (T-bet) and production of the major effector cytokine, IFNγ. T_H1 cells promote response to intracellular pathogens, activation of phagocytes, class switching of B cells to IgG2a and IgG3, and delayed-type hypersensitivity responses (58).

Naïve $CD4^+$ T cells activated in the presence of IL-4 differentiate into T_H2 cells. The IL-4 receptor signals through STAT6 and induces transcription of the T_H2 master transcription factor, GATA3 (57). T_H2 cells are distinguished by their production of IL-4, IL-5, and IL-13, and they function to induce extracellular pathogen responses, B cell class switching to IgG1 and IgE, and eosinophil activation (58).

Regulatory T cells (T_{reg}), as their name implies, function to downregulate effector T cell responses. They come in two flavors, natural T_{reg} and induced T_{reg} (nT_{reg} and iT_{reg} respectively) (59). nT_{reg} differentiate during thymic selection when there is sufficient avidity between self-pMHCII and TCR. iT_{reg} differentiate in the periphery in the presence of TGFβ and IL-2. In addition, retinoic acid potently synergizes iT_{reg} polarization. Forkhead box P3 (FoxP3) is the master regulator and IL-10 is the main cytokine of both nT_{reg} and iT_{reg}, though several other soluble and surface mediators are involved (60). There are also two additional inducible $CD4^+$ T cell subsets with regulatory function. T_R1 cells are $FoxP3^-$, require IL-10 to differentiate, and produce IL-10 and TGFβ (61), while iT_R35 cells are also $FoxP3^-$, require IL-10 and IL-35 to differentiate, and produce IL-35 (62).

The critical finding that IL-23 was essential for development of experimental autoimmune encephalomyelitis ultimately led to the discovery of T_H17 cells (63). IL-23, it turns out, is required for the maintenance of T_H17 cells. This lineage of T helper cells occurs when naïve T cells are activated in the presence of proinflammatory IL-6 or IL-21 and anti-inflammatory TGFβ. This induces transcription of the master regulator RAR-related orphan receptor gamma, isoform t (RORγt). T_H17 cells secrete autocrine IL-21 and IL-23 to ramp up and maintain RORγt expression, and IL-17 and IL-22 as effector

cytokines. Their main function is to mediate immunity toward extracellular pathogens by recruiting neutrophils and inducing local antimicrobial responses by stromal tissues (64).

It is also worth mentioning that, in addition to these four subsets, additional $CD4^+$ T helper cell lineages have been discovered in recent years. $CD4^+$ T cells that are activated in the presence of IL-4 and TGFβ differentiate into IL-9 producing T_H9 cells (65, 66). Like T_H17 cells, T_H22 cells produce IL-22 but appear to be a distinct subset in that they do not secrete IL-17 (67, 68). Located in germinal centers (GC), T_{FH} cells are required for GC formation and maintenance, and are noted for expression of their master transcription factor B-cell CLL/lymphoma 6 (Bcl6) and of the GC homing cytokine chemokine (C-X-C motif) receptor 5 (CXCR5) (69). While they do produce IL-21, which aids B cell class switching in GCs, they also are capable of IFNγ, IL-4, and IL-17 production. Thus, they are not characterized by a canonical cytokine per se, and it is not clear if they are actually T_H1, T_H2, and T_H17 cells whose receptor affinity has allowed them to further differentiate into T_{FH}.

T_H1 in SLE

Upon the initial identification and functional description of the T_H1 and T_H2 subsets, the dogma soon developed that cell-mediated autoimmune disorders, such as type 1 diabetes, were T_H1 mediated, while humoral autoimmune disorders, such as SLE, were T_H2 mediated. Since then, evidence has mounted demonstrating a major role for T_H1 cells in SLE pathogenesis (58). It was, in fact, several years before the description of T_H1 cells that high levels of IFNγ in the sera of SLE patients was first found to positively correlate with disease severity indicators anti-DNA antibodies and low C3 (70). More recently, similar findings reported greater numbers of peripheral cells from SLE patients produce IFNγ than from healthy controls (71). In addition, more of

the T_H1-inducing cytokines, IL-12 and IL-18, are found in the serum, glomeruli, and urine from SLE patients, and IFNγ, IL12, and IL-18 all correlate with the severity of GN (71-73).

The T_H1 association with SLE is reflected in several animal models as well. Increased IFNγ production in NZB/W F1 mice correlates with increased autoantibody levels and GN, while deletion of the IFNγ receptor in these mice prevents these phenotypes (74, 75). Also, $CD4^+$ T cells from mice congenic for the NZW derived *Sle1* locus produce more IFNγ in response to histone-derived pMHCII stimulation than cells from non-congenic mice, showing that increased IFNγ can specifically be a property of autoreactive T cells (43). In MRL/*lpr* mice, the findings were analogous to those in NZB/W F1 mice: more $CD4^+$ T cells produced IFNγ and this, resulting in increased spontaneous and T dependent production of T_H1-induced IgG2a and IgG3 antibodies (76). Finally, the pristane-induced model of SLE is also characterized by requirement for T_H1 since $IFN\gamma^{-/-}$ mice do not develop disease (77).

While it is not certain why increased IFNγ is so strongly associated with disease severity, the class switching to IgG2a and IgG3 that is induced by T_H1 cells is likely to play a role. These isotypes are considered to be more pathogenic because, as opposed to T_H2-induced IgG1, T_H1-induced IgG2a and IgG3 are capable of fixing complement, and can therefore cause more inflammation and tissue destruction (78). Taken together, T_H1 are vital to the pathology of SLE, and thus targeting their dysregulation may prove to be therapeutically beneficial.

T_H17 in SLE[1]

As previously mentioned, the role of T_H17 in the development of autoimmunity was initially scrutinized in murine models of induced EAE (79). This disease model was originally believed to be dependent on IL-12, and thus, T_H1 mediated. However, the revelation that IL-12 shared a subunit, p40, with a newly discovered cytokine, IL-23, and that this novel cytokine, not IL-12, was required for induction of disease set the stage for investigation of T_H17 in these models (63, 80). More recently, several lines of research have reported increased IL-17 production and T_H17 functions in murine models of lupus as summarized Table 1-2.

IL-17 in murine lupus

BXD2 is one of 20 BXD recombinant inbred strains derived from a cross between C57BL/6J (B6) and DBA/2J (81, 82). These mice develop a spontaneous and age-dependent lupus-like syndrome denoted by production of the canonical anti-DNA, anti-histone, and rheumatoid factor autoantibodies, as well as splenomegaly, glomerulonephritis (GN), and erosive arthritis (83, 84). $CD4^+$ T cells from BXD2 mice have enhanced T_H17 development and consequent increased serum levels of IL-17 (85). Moreover, IL-17-secreting $CD4^+$ cells were shown to localize to germinal centers (GCs) in BXD2 spleens. This augmented IL-17 response was associated with increase GC development and stability in BXD2 spleens as compared to B6 controls. Additionally, BXD2 have increased amounts of $IL\text{-}17R^+$ B cells (85). These B cells have both an increased basal and an IL-17R-induced activation of the canonical NFκβ pathway, resulting in an increased expression of regulator of G signaling (RGS) proteins

[1] Reprinted with permission from Arthritis – Hindawi Publishing Company, © 2011 Daniel Perry et al. "The current concept of TH17 cells and their expanding role in Systemic Lupus Erythematosus"

(86). Consequently, RGSs enhance the GTPase activity of chemokine receptor Gα subunits resulting in decreased chemotaxis (87, 88). Indeed, BXD2 B cells were shown to have a diminished chemotactic response to CXCL12 and CXCL13, especially in the presence of IL-17 (85, 86). This increased potential for B cell accumulation at the sites of CXCL12 and CXCL13 production, such as follicular dendritic cell rich areas (89, 90), is the likely cause of the enhanced GC formation in the BDX2 strain. Moreover, the concurrent production of IL-17 by T_H17 cells in GCs further promotes B cell accumulation and GC stability. IL-17 also results in increased activation-induced cytidine deaminase (*Aicda*) expression and somatic hypermutation in BXD2 IL-17R$^+$ B cells, which have an intrinsically enhanced ability to produce autoantibodies as compared to IL-17R deficient BDX2 B cells (85). Thus IL-17 has a central role in pathogenesis of the lupus-like syndrome observed in this model.

The MRL/*lpr* strain is a classical model of spontaneous lupus. It exhibits a lymphoproliferative disorder which manifests with autoantibody production, GN and accumulation of CD4$^-$CD8$^-$ double-negative T (DNT) cells in the periphery (91). A mutation in *Fas* is responsible for the *lpr* phenotype and is the major functional contributor of pathogenesis in this strain (92, 93). It was recently shown that *Fas*-deficient DNT cells are capable of producing significant amounts of IL-17 (94). Further, the T_H17-stablizing cytokine, IL-23, potently induced IL-17 production in these DNT cells that were then capable of renal infiltration and GN induction. Finally, deletion of IL-23R prevented splenomegaly, lymphadenopathy, autoantibody production, and GN in the context of *Fas* deficiency and was associated with a major reduction of the DNT cell compartment along with its concomitant IL-17 production (95). Thus, a pathogenic

TH17-like function of DNT cells has been exposed, highlighting this subset as a target for disease intervention.

The SNF1 mouse model, derived from the F1 outcross of the New Zealand Black and SWR recombinant inbred strains, develops a spontaneous lupus-like syndrome that can be accelerated by immunization of nucleosomal peptides (96). Upon disease induction, autoantibodies are produced and GN with TH17 infiltration is initiated (97). Interestingly, low-dose therapy of a tolerogenic histone-derived peptide caused increased TGF-β and decreased IL-6 expression in dendritic cells and resulted in enhancement of Treg function with a reduction in TH17 renal infiltrates (97). Treatment with either oral or nasal anti-CD3 also ameliorated autoantibody production and nephritis in this model by inducing a regulatory T cell subset and reducing IL-17 production by T follicular helper cells (98, 99). These results indicate that therapies regulating T_{reg}/T_H17 homeostasis in favor of T_{reg} might be effective at moderating SLE pathogenesis.

Finally, disruption of TNF-α receptor signaling in spontaneous lupus-prone NZM2328 mice results in exacerbated disease that associated with a greatly enhanced T effector/memory compartment. These cells were found to have a T_H17 gene signature and produced more IL-17 than TNF-α receptor sufficient T effector/memory cells (100). This work highlights a TNF-α regulatory function and raises a note of caution for TNF-α blockade therapy.

IL-17 in SLE patients

As with murine lupus models, evidence for a T_H17 role in human SLE is also mounting. Several recent reports show that plasma IL-17 and IL-17 producing T cells are increased in SLE patients (101-106). Moreover, disease activity and severity is

associated with increased IL-17 production (101-104). SLE patients have increased phosphorylation of STAT3 (107), which is required for T_H17 differentiation, as STAT3 deficiency in hyper IgE syndrome patients results in the ablation of T_H17 cells (108, 109). The T_H17-polarizing cytokines, IL-6, IL-21, and IL-23, all signal in a STAT3-dependent manner to induce RORγt production (110). Indeed, SLE patients also have increased plasma levels of IL-6, and higher *RORC* expression, which encodes RORγt (102, 111). Taken together, T_H17 expansion is an important feature of SLE that needs to be further investigated.

Since IL-17 production correlates with disease severity, the question is raised as to whether the female bias of SLE is due to differences in T_H17 biology. While this has not been studied extensively, production of IL-17 *in vitro* was shown to decrease with age in men, but not in women (112). Although these results do demonstrate a gender difference, the relevance to SLE induction is not clear since the young cohorts, who were between 21 and 40 years old (the highly susceptible age of onset for SLE) did not produce different amounts of IL-17 in males versus females. Nevertheless, the ability to maintain higher levels of IL-17 production with age may contribute to the maintenance of the disease state in females. More recently, it was reported that *in vivo* treatment of mice with estrogen enhances T_H17 polarization *in vitro*, supporting the hypothesis that T_H17 cells contribute to the female bias of SLE (113). There is, however, no direct evidence for this theory and further study is needed to clarify the role that gender may play in T_H17 function and disease induction.

Similar to *Fas* deficient mouse models of lupus, a significant amount of IL-17 is also produced by an expanded subset of DNT cells in SLE patients (105). These DNT

cells are derived from $CD8^+$ cells that have downregulated CD8 in response to receptor stimulation (114). While they are normally present in very small amounts, their expansion in SLE patients may be due to increased T cell activation. Because of their downregulated co-receptor, they have decreased survival and proliferation and display unique gene expression patterns and proinflammatory cytokine profiles (114). Notably, as in lupus-prone mice, DNT cells can be found in kidney biopsies of SLE patients (105). Therefore, DNT cells appear to represent a distinct effector population of T cells whose dysregulation may be central to SLE pathogenesis.

The fundamental role of type I IFN dysregulation is well established in SLE pathogenesis (7). Unregulated IFN-α production has been shown to increase proinflammatory cytokine production, including for IL-6 and IL-23 that lead to T_H17-mediated inflammation in mice (115). Also plasmacytoid dendritic cells (pDCs), which are known to potently secrete IFN-α, also produce IL-1β, IL-6, and IL-23 in response to Toll-like receptor (TLR)-7 stimulation in human studies (116, 117). These pDCs are capable of inducing T_H17 differentiation when co-cultured with $CD4^+$ cells. Endogenous nucleic acids are autoantibody targets in SLE and are capable of TLR activation following their uptake as immune complexes (1, 118). Therefore, pDCs can be chronically activated, potentiating T_H17 development and disease pathogenesis.

IL-17 also promotes B cell survival both alone and synergistically with B cell-activating factor (BAFF) (104). Hence, a feedback loop is established where IL-17 promotes autoreactive B cells to persist longer and make autoantibodies which activate pDCs to induce more T_H17 cells. In parallel, the expansion of DNT cells results in more IL-17 production, exacerbating this progression (Figure 1-3). As IL-17 is a central

mediator to this process, therapeutic intervention that targets T_H17 development and IL-17 production will be valuable treatments for SLE.

Table 1-1. 1997 Update of the 1982 American College of Rheumatology Revised Criteria for Classification of Systemic Lupus Erythematosus (3, 4)

Criterion	Description
1. Malar Rash	Fixed erythema, flat or raised, over the malar eminences, tending to spare the nasolabial folds
2. Discoid rash	Erythematous raised patches with adherent keratotic scaling and follicular plugging; atrophic scarring may occur in older lesions
3. Photosensitivity	Skin rash as a result of unusual reaction to sunlight, by patient history or physician observation
4. Oral ulcers	Oral or nasopharyngeal ulceration, usually painless, observed by physician
5. Nonerosive Arthritis	Involving 2 or more peripheral joints, characterized by tenderness, swelling, or effusion
6. Pleuritis or Pericarditis	1. Pleuritis--convincing history of pleuritic pain or rubbing heard by a physician or evidence of pleural effusion OR 2. Pericarditis--documented by electrocardigram or rub or evidence of pericardial effusion
7. Renal Disorder	1. Persistent proteinuria > 0.5 grams per day or > than 3+ if quantitation not performed OR 2. Cellular casts--may be red cell, hemoglobin, granular, tubular, or mixed
8. Neurologic Disorder	1. Seizures--in the absence of offending drugs or known metabolic derangements; e.g., uremia, ketoacidosis, or electrolyte imbalance OR 2. Psychosis--in the absence of offending drugs or known metabolic derangements, e.g., uremia, ketoacidosis, or electrolyte imbalance
9. Hematologic Disorder	1. Hemolytic anemia--with reticulocytosis OR 2. Leukopenia--< 4,000/mm3 on ≥ 2 occasions OR 3. Lyphopenia--< 1,500/ mm3 on ≥ 2 occasions OR 4. Thrombocytopenia--<100,000/ mm3 in the absence of offending drugs
10. Immunologic Disorder	1. Anti-DNA: antibody to native DNA in abnormal titer *OR* 2. Anti-Sm: presence of antibody to Sm nuclear antigen *OR* 3. Positive finding of antiphospholipid antibodies on: a. an abnormal serum level of IgG or IgM anticardiolipin antibodies, b. a positive test result for lupus anticoagulant using a standard method, or c. a false-positive test result for at least 6 months confirmed by Treponema pallidum immobilization or fluorescent treponemal antibody absorption test
11. Positive Antinuclear Antibody	An abnormal titer of antinuclear antibody by immunofluorescence or an equivalent assay at any point in time and in the absence of drugs

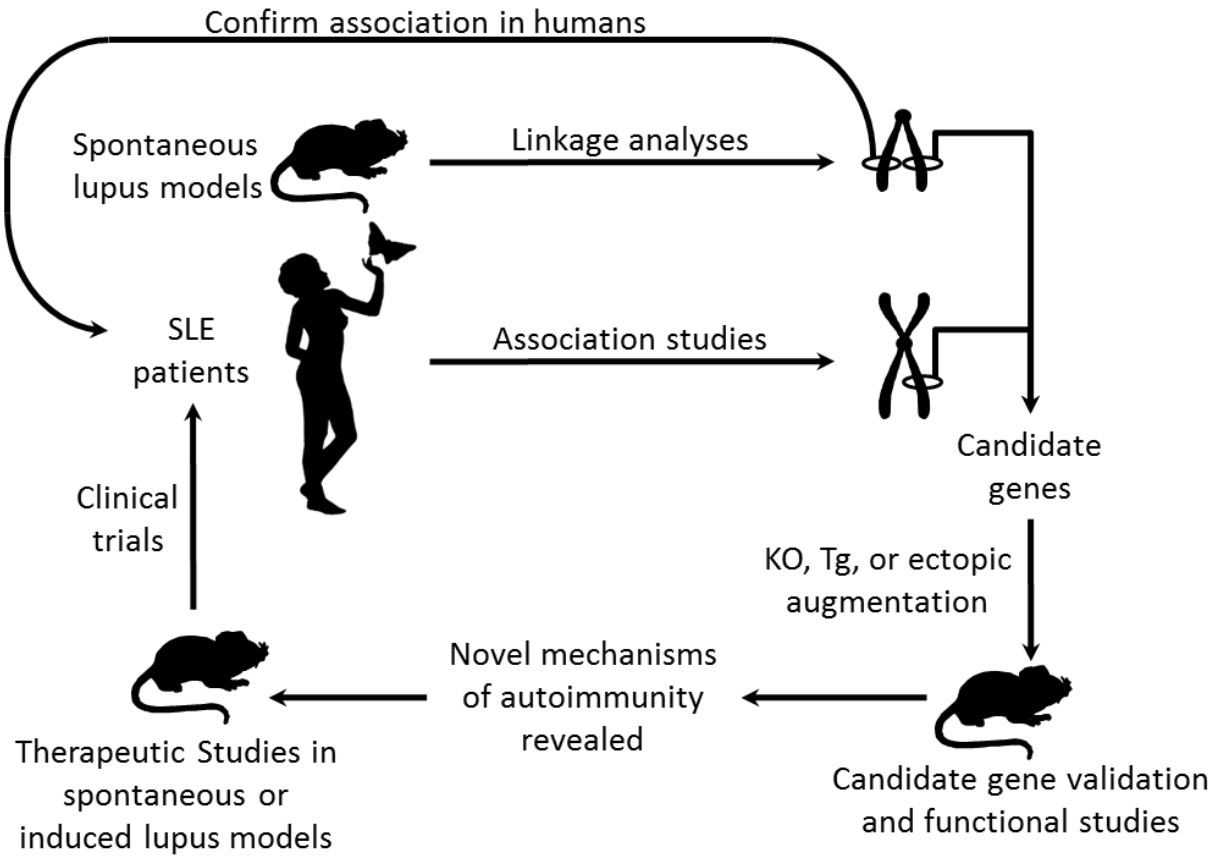

Figure 1-1. Integration of human and murine studies for new SLE drug discovery. Study of human SLE patients and mouse models of lupus has led to the identification of potential therapeutic targets. In-depth studies in murine models are undertaken to validate the association of the potential targets with disease symptoms. The efficacy of targeted treatments is first tested on murine models of lupus prior to the initiation of human clinical trials.[2]

[2] Reprinted with permission from Journal of Biomedicine and Biotechnology – Hindawi Publishing Company, © 2011 Daniel Perry et al. "Murine Models of Systemic Lupus Erythematosus"

Figure 1-2. Map of the *Sle1c* locus at the beginning of the project. All MIT microsatellite markers are shown, where black denotes a polymorphic and gray a non-informative marker for B6 and NZW. Positions of known protein coding genes are shown. The recombination interval is between *D1MIT459* and *D1MIT274*.

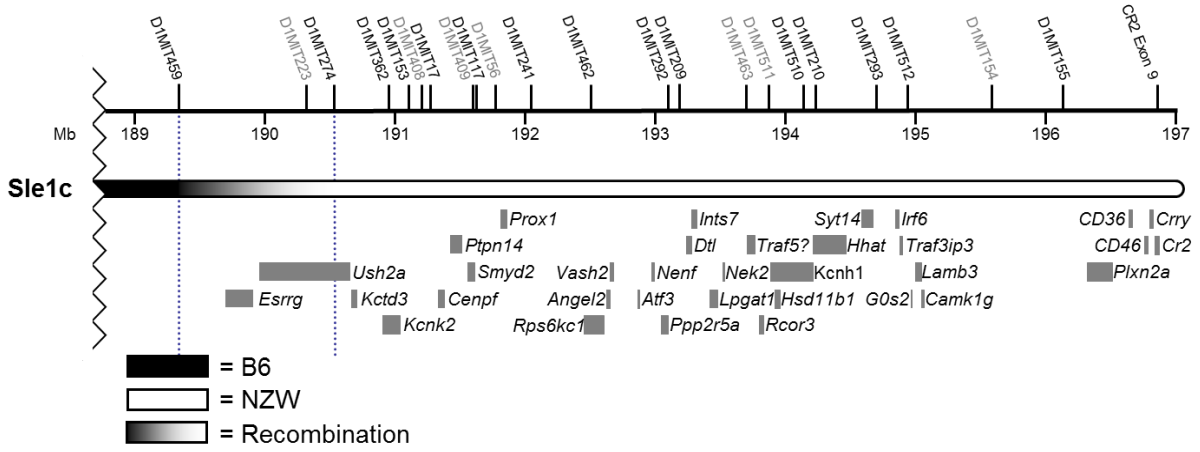

Table 1-2. IL-17 in murine models of lupus.[3]

Model	Description	References
BXD2	IL-17 promotes spontaneous GC development as well as autoantibody production by IL-17R$^+$ B cells	(85, 86)
MRL.*lpr*	Expansion of IL-17-producing DNT cells with kidney infiltration and GN induction	(94, 95)
SNF1	Enhanced IL-17 production by CD4$^+$ T cells with kidney infiltration	(97)
NZM2328	Disruption of TNFα promotes Th17 development	(100)

[3] Reprinted with permission from Arthritis – Hindawi Publishing Company, © 2011 Daniel Perry et al. "The current concept of TH17 cells and their expanding role in Systemic Lupus Erythematosus"

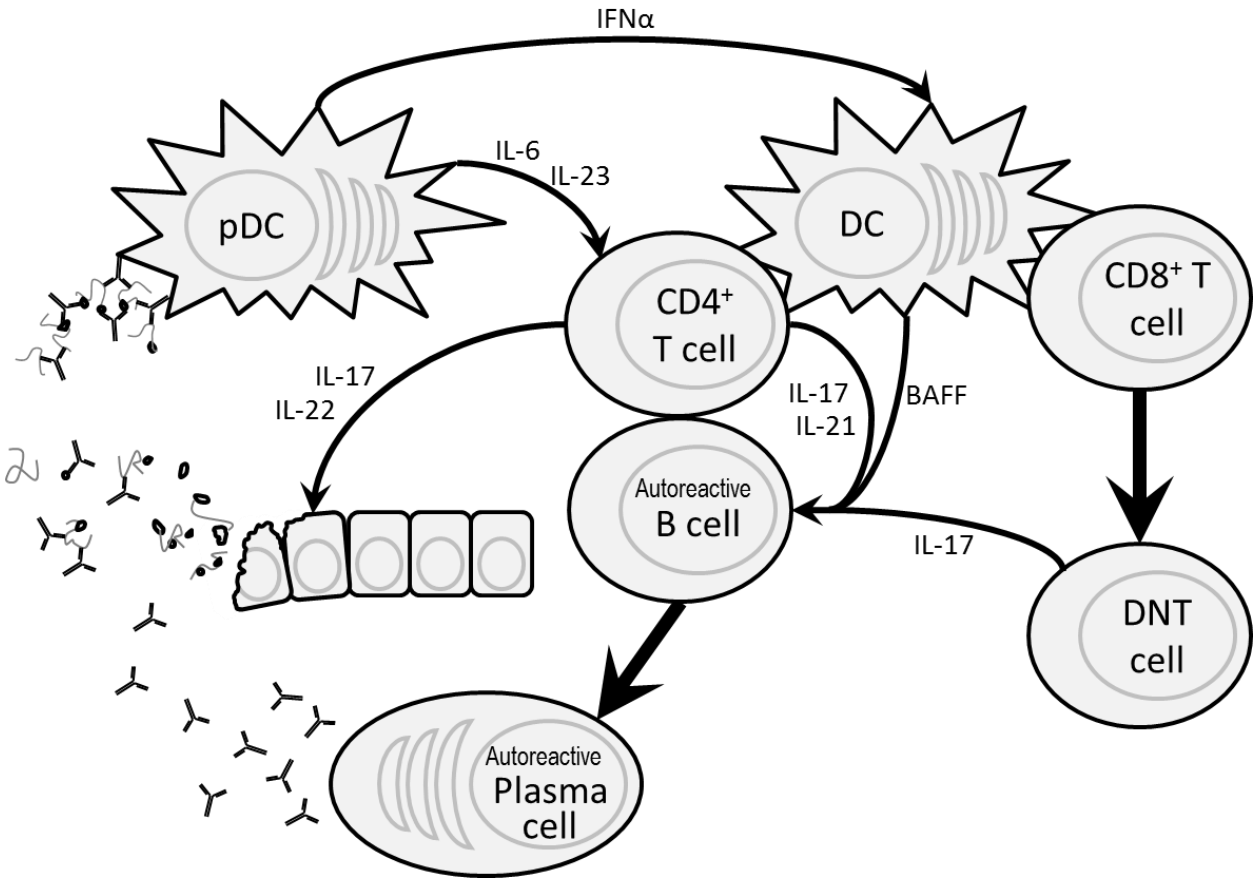

Figure 1-3. IL-17 in SLE pathogenesis. IL-17, IL-21, and BAFF promote survival, class-switching, and production of antinuclear autoantibodies by autoreactive B cells. Consequently, nucleic acid-containing immune complexes stimulate pDCs to produce type I interferon, IL-6, and IL-23, which enhance DC activation, and T_H17 induction, thus completing a feedback loop for autoimmune activation. Concurrently, hyperactivation in the context of autoimmunity may actuate the accumulation of DNT cells that produce more IL-17 and exacerbates the disease state. Ultimately, T_H17 and DNT cells infiltrate systemic tissues and incite end organ disease.[4]

[4] Reprinted with permission from Arthritis – Hindawi Publishing Company, © 2011 Daniel Perry et al. "The current concept of TH17 cells and their expanding role in Systemic Lupus Erythematosus"

CHAPTER 2
MURINE LUPUS SUSCEPTIBILITY LOCUS *SLE1C2* MEDIATES $CD4^+$ T CELL HYPERACTIVATION AND MAPS TO ESTROGEN RELATED-RECEPTOR GAMMA *ESRRG*

To review from chapter 1, patients afflicted with SLE suffer an assortment of symptoms that can affect any organ system and that vary in nature and severity throughout disease progression. The most common indicator of SLE is the presence of antinuclear autoantibodies (ANA) that aberrantly target nuclear antigens, such as double-stranded DNA (dsDNA), histone and chromatin complexes, and ribonucleoproteins. The resultant immune complexes then aggregate in basement membranes, triggering inflammation and tissue damage. A common complication of SLE occurs when this process takes place in the kidney, a condition known as glomerulonephritis (GN), leading to kidney failure and death. The murine NZM2410 recombinant inbred strain spontaneously develops a lupus like disease that closely mimics SLE in humans. Derived from the classic NZB/W F1 murine lupus model, it has an advantage over its parental strains in that it is homozygous, making it an ideal model to identify novel genetic determinants of lupus (reviewed (47, 119). Linkage analysis of NZM2410 to GN identified the major lupus susceptibility locus, *Sle1*, as an NZW-derived interval on Chromosome 1 beginning at *D1MIT30* and extending to the telomere (34). This region overlaps syntenic human SLE QTLs, 1q22-23 and 1q41-42, suggesting that similar genetic factors mediate pathogenesis in both species (44)}. Subsequent studies using congenic mice demonstrated distinct functional requirements that *Sle1* imparted in the induction of murine lupus. Specifically, B6.*Sle1* mice display B and T cell intrinsic loss of tolerance to nuclear antigens (35, 43, 120, 121). Still, the underlying genetic

determinants of SLE pathogenesis remained obscure in this 62Mb region, which contains an estimated 350 genes.

The challenging process of candidate gene identification employed extensive phenotypic mapping and has so far revealed that at least five genes are responsible for the *Sle1* phenotype. Initially, three subloci, *Sle1a*, *Sle1b*, and *Sle1c*, were found to contribute to the production ANA, revealing the complex genetics of this locus (50). Then *Sle1a* and *Sle1c* were themselves determined to correspond to at least two subloci, yielding *Sle1a1*, *Sle1a2*, *Sle1b*, *Sle1c1*, and *Sle1c2* as the five current subloci of *Sle1* (52, 122). Complement receptor 2 (*Cr2*) was the first candidate gene for *Sle1c* and subsequently found to co-segregate with the telomeric *Sle1c1* (52, 53). Ensuing human association studies confirmed these findings by identifying a haplotype that alters *CR2* splicing (123, 124). Additionally, the effect of *Sle1b* has been attributed to polymorphisms in the signaling lymphocytic activation molecule (SLAM)/CD2 gene cluster, with direct evidence for one SLAM family member, *Ly108* (29, 30). Finally, though not yet validated, pre B-cell leukemia transcription factor 1 *Pbx1* is the only positional candidate for *Sle1a1* (122). Thus, three novel lupus susceptibility candidate genes have been identified within the *Sle1* interval.

T cell hyperactivation and dysregulation of their effector cytokines are central to SLE pathogenesis, thus they are ideal targets for novel therapies (125, 126). We have previously reported that a sublocus at the centromeric end of *Sle1c*, termed *Sle1c2*, is associated with increased activation and proliferation of $CD4^+$ T cells (52). In this chapter, I describe the mapping of *Sle1c2* to Estrogen-related receptor gamma (*Esrrg*) gene, which encodes a nuclear receptor (ERRγ) whose ligand binding pocket and

regulation of transcriptional programs make it a therapeutic candidate. Additionally, I further characterize effector responses and identify an expansion of IFNγ secreting T_H1 cells in congenic B6.*Sle1c2* mice. Finally, I demonstrate the pathogenicity of these traits in two lupus accelerating disease models.

Materials and Methods

Mice

B6.*Sle1c* mice that contain a NZW-derived congenic interval at the telomere of Chromosome 1 have been described previously (50). The loci previously referred to as *Sle1c.Cr2^{w}-1* and *Sle1c.Cr2^{b}-1* in that a previous study (52) have been renamed *Sle1c1* and *Sle1c2* respectively to be more consistent with the terminology of other loci. To generate subcongenic strains, B6 x B6.*Sle1c* F1 mice were backcrossed to B6 and the progeny were tested for recombinations in the *Sle1c* interval by genotyping microsatellites that are polymorphic between NZW and B6. Individuals that were positive for recombinations were bred to B6 and the progeny of this expansion backcross were screened for the subcongenic interval as above and then bred to homozygosity. To fine map the ends of congenic intervals, positional SNPs that are polymorphic for B6 and NZW were selected from Mouse Phenome Database (http://phenome.jax.org/SNP) and flanking primers were used in BigDye Terminator (ABI) sequencing reactions to determine alleles. B6.Cg-Tg(TcraTcrb)425Cbn/J (B6.OTII) (127) and B6(C)-H2-Ab1^{bm12}/KhEgJ (B6.bm12) were purchased from The Jackson Laboratory. B6.FoxP3-eGFP knock-in mice (128) were a kind gift from Vijay Kuchroo. Bicongenic B6.*Sle1c2* mice containing the OTII transgene or the FoxP3-eGFP knock-in locus were generated as above. B6.129P2-Tcrb^{tm1Mom}Tcrd^{tm1Mom}/J (B6.*Tcrbd$^{-/-}$*), B6.129S2-Ighm^{tm1Cgn}/J (B6.*Mu*MT) and B6.Cg-Igh^{a}Thy1^{a}Gpi1^{a}/J

(B6.*Thy1*^{a}) mice were purchased from The Jackson Laboratory and used for mixed bone marrow experiments. NZB mice were purchased from The Jackson Laboratory and used to generate B6 x NZB F1 and B6.*Sle1c2* x NZB F1. All mice were bred and maintained at the University of Florida in specific pathogen-free conditions. All experiments were conducted according to protocols approved by the University of Florida Institutional Animal Care and Use Committee.

Cell Isolation and Culture

Single cell suspensions were prepared by mechanically disrupting spleen and lysing red blood cells in 155mM NH_4Cl for 3 minutes at room temperature. Cells were then washed in ice cold 5% FCS in PBS and passed through 30µm nylon mesh to remove debris. Splenocyte suspensions were enriched for $CD4^+$ T cells by labeling with magnetic beads and negatively selecting on magnetic columns using $CD4^+$ T cell Isolation Kits (Miltenyi) per manufacturer's protocol. To sort $CD4^+$ cells into Naïve and T_{em} populations, splenocytes from 3 mice were first enriched for $CD4^+$ T cells as above and pooled, then labeled with fluorescently conjugated antibodies againstCD4, -CD62L, and CD44 and sorted (Naïve: $CD4^+CD44^{lo}CD62L^+$ and T_{em}: $CD4^+CD44^{hi}CD62L^-$) by a FACSAria cell sorter (BD Biosciences). RPMI supplemented with 10% FCS, HEPES, 2-Mercaptoethanol, and penicillin-streptomycin was used as culture medium. Cells were stimulated either with plate-bound antibody, by pre-coating with 5µl/ml anti-CD3e (145-2C11) and 2.5µl/ml anti-CD28 (37.51) in PBS, or with 0.5µg/ml phorbol 12-myristate 13-acetate and 1µM ionomycin. For antigen-specific proliferation assays, total splenocytes from B6 mice were irradiated with 2000Rad and pulsed for 2 hours at 37°C with either $OVA_{323-339}$ or H_{476-90} at the indicated concentrations. These were then co-cultured 1:1 with bead-enriched $CD4^+$ T cells from OTII mice in triplicate. ^{3}H-Thymidine was added

at 1μCi/200μl for the last 18 hours of 72-hour cultures to measure proliferation. Cells were then harvested onto glass filter paper and counts per minute were measured using a liquid scintillation counter. For T_H17 polarization, $CD4^+$ T cells were cultured with plate-bound anti-CD3e and anti-CD28, 2.5ng/ml TGF-β, and 25ng/ml IL-6 for 48 hours. For Treg culture, FACS sorted $CD4^+GFP^-$ T cells from FoxP3-eGFP mice were cultured with plate-bound anti-CD3e and anti-CD28, and 2.5ng/ml TGF-β with or without 10nM all-trans-retinoic acid (atRA).

Flow Cytometry

Cell suspensions were blocked with 10% normal rabbit serum and anti-CD16/32 (2.4G2) in staining buffer (5% FCS, 0.05% sodium azide in PBS) and incubated on ice for 30 minutes. Biotinylated or fluorophore-conjugated antibodies specific for CD3 Molecular Complex (17A2), CD4 (RM4-5), CD8a (53-6.7), CD44 (IM7), CD62L (MEL-14), CD25 (7D4), CD69 (H1.2F3), CD90.1 (OX-7), CD90.2 (53-2.1), B220 (RA3-6B2), CD19 (1D3), IgM (II/41), CD80 (16-10A1), CD86 (GL1), I-Ab (AF6-120.1), and isotype controls were used in predetermined amounts and combinations for surface staining by incubating on ice for 1 hour. When needed, streptavidin-peridinin chlorophyll-a protein-Cy5.5 (SA-PerCP-Cy5.5, BD Biosciences) was used to detect biotinylated antibodies by incubating on ice for 20 minutes after primary antibodies were washed off. IFNγ (XMG1.2), IL-4 (11B11), IL-17A (TC11-18H10), and FoxP3 (FJK-16s) were detected using Fixation/Permeabilization kits (eBiosciences) per manufacturer's protocol. All antibodies were from BD Biosciences except for anti-FoxP3, which was from eBiosciences. After staining, cell suspensions were washed and stored in staining buffer with 1% formalin at 4°C until analysis on a FACSCalibur cytometer (BD Biosciences). At least 50,000 events per sample were collected and lymphocyte

populations were gated based on forward and side scatter characteristics. When cytokine profiles were analyzed, cells were treated with leukocyte activation cocktail (BD Biosciences) prior to staining per manufacturer's protocol.

Gene Expression Analyses

Total cellular RNA from prepared cell suspensions, cerebrum, liver, heart, and kidney was isolated using RNeasy mini kits, Qiashredders, and RNase-free DNase sets (Qiagen). cDNA was then synthesized using the ImProm-II Reverse Transcription System (Promega). Primers for potential ERRγ target genes were designed using Primer3 software (129) and tested for specific generation of desired amplicons using standard PCR. Suitable primers (Table 2-1) were used in Sybr Green (Applied Biosystems) based Real Time PCR. Taqman Gene Expression Assays (Applied Biosystems) were used to measure *Esrrg* (Mm00516269_mH) and *Gapdh* endogenous control. Relative quantities were calculated using the comparative C_T method ($RQ=2^{-\Delta\Delta Ct}$) normalized to the average ΔC_T of the B6 biogroup. Global gene expression of $CD4^+$ T cells from 6 month old B6 and B6.*Sle1c2* mice (n=5 per strain) began with RNA isolation from bead-sorted splenocytes as above. Next, cDNA was synthesized, fragmented, and biotin-labeled using the Ovation Biotin RNA Amplification and Labeling System (NuGEN Technologies). Finally, prepared cDNA was hybridized to Affymetrix Mouse Genome 430 2.0 arrays. All data analyses were based on the use of "internal standards" and generalization of the "Error Model" (130) as presented elsewhere (131).

ELISA

Anti-dsDNA and anti-chromatin were measured by ELISAs as previously described (43). Sera were tested in duplicate in a 1:100 dilution. Relative units were

standardized using a positive serum from an NZM2410 mouse, arbitrarily setting the reactivity of a 1:100 dilution of this control serum to 100 units.

Western Blot

To detect ERRγ, cells were washed in PBS, lysed by resuspending and vortexing in ice-cold RIPA-lysis buffer (50mM NaF, 2mM activated sodium orthovanadate, 2mM PMSF, 2µg/ml aprotinin, 10µg/ml leupeptin, and 1µg/ml pepsatin A, 1% Nonidet P-40, 0.5% sodium deoxycholate, 1% SDS in PBS; all reagents from Sigma), and aggregates were removed by centrifugation. The protein concentrations of homogenates were quantified using a Bradford Assay (Bio-Rad). Total proteins (50µg) were boiled for 5 minutes in Laemmli buffer, and then separated by SDS-PAGE in 10% gels, followed by transfer to polyvinylidene fluoride membranes. After blocking in 5% milk in TBS-T, membranes were probed with anti-ERRγ mAb (H6812, R&D Systems), followed by Clean-Blot Detection Reagent-HRP (Thermo Scientific), and developed with Amersham ECL Plus Western Blotting Detection Reagent (GE Healthcare).

Mixed Bone Marrow Chimera

Chimeras were prepared as previously described (121). Briefly, 4-5 month old B6.*Tcr*$^{-/-}$ recipients were lethally irradiated with two doses of 525Rad 4-6 hours apart the day before reconstitution. Donor bone marrow cell suspensions from B6.*Thy1*^{a} and B6.*Sle1c2* were mixed 1:1 after depleting T cells using anti-CD5 magnetic microbeads (Miltenyi). Recipients received 10^{7} cells intravenously from sex-matched donors and grafts were allowed to reconstitute for 8 weeks. In a parallel experiment, hosts were 2 month old B6 and donors were B6.*Mu*MT and B6.Tcrbd$^{-/-}$ or B6.*Sle1c2*.*Mu*MT and B6.Tcrbd$^{-/-}$. These chimeras were engineered to have B or T cells of B6.*Sle1c2* origin. After reconstitution, these chimeras were used as cGVHD recipients.

Chronic Graft-Versus-Host Disease (cGVHD)

cGVHD was induced as previously described (132). Briefly, B6 and B6.*Sle1c2* hosts received 8 x 10^7 B6.bm12 splenocytes via i.p. injection. In another experiment, cGVHD was induced in B6.*Mu*MT/B6.*Tcrbd*$^{-/-}$, B6. *Mu*MT/B6.*Sle1c2*.*Tcrbd*$^{-/-}$, and B6.*Sle1c2*.*Mu*MT/B6.*Tcrbd*$^{-/-}$ mixed bone marrow chimeras. Sera were collected weekly for 3 weeks after induction and stored for ELISA. Hosts were sacrificed 3 weeks after transfer, kidneys were prepared for histology, and splenocytes were analyzed by FACS. The presence of immune complexes in the kidneys was evaluated on frozen tissue sections stained with FITC-conjugated anti-C3 (Cappel) and anti-IgG H+L chains (Jackson Immunoresearch). Staining intensity was evaluated in a blind manner on a semi-quantitative 0–3 scale and averaged on at least 10 glomeruli per section.

EAE

Induction of experimental autoimmune encephalomyelitis (EAE), a well-characterized animal model of multiple sclerosis, has been previously described (128, 133). On day 0, four-month-old male B6 or B6.*Sle1c2* mice were anesthetized and treated with an emulsion of 100μg myelin oligodendrocyte glycoprotein (MOG) peptide sequence 35–55 ($MOG_{35–55}$) and 50μg of Mycobacterium tuberculosis in incomplete Freund's adjuvant (equivalent to CFA) via subcutaneous injection to the left of the base of the tail. Additionally, 200ng pertussis toxin was administered intraperitoneally on days 0 and 2. Daily clinical scores were assessed by the following criteria: 0, no disease, 1, flaccid tail, 2, hind limb paraparesis, 3, hind limb paralysis, 4, quadriplegia, 5, moribund. Mice were euthanized at a score of 4 and not allowed to progress to a moribund state.

Statistical Analysis

Statistical analyses were performed using the GraphPad Prism 4 software. Unless indicated, graphs show median values for each group. Mann-Whitney and Student's t-tests were used for direct comparisons and Dunn's and Bonferroni corrections were used for multiple comparisons as indicated. Each *in vitro* experiment was performed at least twice, with reproducible results.

Results

$CD4^+$ T Cell Hyperactivation Maps to the Centromeric End of *Sle1c*

In order to narrow the set of potential candidate genes responsible for the $CD4^+$ T cell hyperactivation displayed by *Sle1c* congenic mice, several subcongenic strains were generated in which recombinations at the centromeric end were targeted using microsatellite markers that are polymorphic between B6 and the parental NZW. Additional fine mapping was performed using polymorphic SNPs. This revealed a 675Kb NZW derived centromeric extension between rs31626695 and rs49456336 in two of the subcongenic strains, REC2b and REC5, and the original B6.*Sle1c* strain (Figure 2-1A). In addition, it redefined the centromeric terminus of *Sle1c* from *D1MIT459* to rs30920616, shortening the locus length to 7.39Mb.

Phenotypic mapping showed that only the strains with this centromeric extension displayed increased spleen weight and CD4:CD8 T cell ratio in aged mice as compared to B6 (Figure 2-2A). Additionally, these strains displayed hyperactivation of the $CD4^+$ T cell compartment as they had a significantly higher percentage of $CD69^+$ activated T cells and of $CD44^{hi}CD62L^-$ T effector/memory cells (T_{em}). Since the strain with the shortest interval necessary for $CD4^+$ T cell hyperactivation is the REC5 subcongenic, and REC1, 2, 3, and 8 are negative, *Sle1c2* is then defined as the region between

SNPs rs30920616 and rs32528185 (Figures 2-1A, 2-1B). Except where noted, REC5 is used as B6.*Sle1c2* for the remainder of this study.

As opposed to the splenomegaly phenotype, which is age-dependent, the $CD4^+$ hyperactivation phenotype is detectable in very young mice (Figures 2-2B, 2-3A), indicating a more direct effect of the *Sle1c2* interval for this phenotype. Importantly, as previously shown for the entire *Sle1c* interval (52), mixed bone marrow chimera experiments show that $CD4^+$ hyperactivation is intrinsic to *Sle1c2* T cells (Figure 2-3B). As expected, the previously observed increased proliferation of B6.*Sle1c* $CD4^+$ T cells also co-segregated with the *Sle1c2* interval (Figure 2-2C). This inherent hyperactivation and resultant proliferation results in an overall expansion of the $CD4^+$ T cell compartment, specifically T_{em}, not naïve $CD4^+$ T cells (Figure 2-2B). Modest age-dependent expansions of B cell and $CD8^+$ T cell compartments were also observed in B6.*Sle1c2* mice (Figure 2-2B), however, surface phenotype analysis found no evidence of hyperactivation in these cells (not shown). Taken together, the $CD4^+$ T cell hyperactivation phenotype observed in mice congenic with the 7.39Mb NZW-derived *Sle1c* interval has been shown to co-segregate with the much shorter 675Kb *Sle1c2* interval. This drastically reduces the set of potential candidate genes from 48 to 2 (Figure 2-1B).

Sle1c2 Exhibits a Unique Cytokine Profile Denoted by Marked T_H1 Skewing

A gene expression and pathway analysis of B6 and B6.*Sle1c2* $CD4^+$ splenocytes revealed a large node of upregulated genes related to INFγ expression, indicating a T_H1 skewing in B6.*Sle1c2* mice (Figures 2-4A, 2-4B). Intracellular staining of splenocytes confirmed this finding, as a much larger percentage of $CD4^+$ splenocytes from B6.*Sle1c2* were $IFN\gamma^+$ as compared to B6 (Figure 2-5A). No differences were observed

in percentages of IL-4 production. In addition to IFNγ, several genes involved in T_H17/T_{reg} homeostasis were upregulated in B6.*Sle1c2* $CD4^+$ T cells (Figure 2-5B). These included genes encoding the master transcription factor, Forkhead Box P3 (*FoxP3*), a major surface marker, interleukin 2 receptor α (*Il2ra*), and a major effector cytokine, (*IL10*), for T_{reg} cells (134), as well as the required transcription factors, interferon regulatory factor 4 (*Irf4*) and RAR-related orphan receptor alpha (*Rora*), and effector cytokines, *Il17a*, *IL21*, and *Il22*, for T_H17 cells (64). Additionally, the aryl hydrocarbon receptor (*Ahr*), which has been implicated in T_H17/T_{reg} homeostasis (135) was also upregulated.

In spite of this marked T_H17/T_{reg} signature, *in vitro* and *in vivo* analyses did not reveal a propensity to favor either of these subsets. Incorporation of a FoxP3-eGFP reporter allele (128) in B6 and B6.*Sle1c2* mice showed that, contrary to our previous reports that measured T_{reg} as $CD4^+CD62L^+CD25^+$ (52, 136), there is a slight age–dependent accumulation of T_{reg} (Figure 2-3C). However, B6.*Sle1c2* $CD4^+GFP^-$ T cells cultured in the presence of TGFβ with or without all-trans-retinoic acid (atRA) had an unaltered percentage of FoxP3 expressing cells (Figure 2-3D). To measure T_H17 polarization, $CD4^+$ cells were cultured with TGFβ and IL-6. This also did not reveal differences in IL-17 production between the two strains (Figure 2-5C). Finally, EAE was used as model to test for differences in T_H17/T_{reg} homeostasis *in vivo* (137), and once again, no differences were observed in day of onset or severity (Figure 2-5E). Notably, IFNγ production by B6.*Sle1c2* $CD4^+$ T cells was increased *in vitro*, especially under T_{reg} and T_H17 polarizing conditions (Figure 2-5C), highlighting the T_H1 skewing induced by *Sle1c2*. Hence, while the global gene expression analysis predicted increased

commitment to T_H1, T_{reg}, and T_H17 lineages, the only observed difference was with T_H1 cells.

Esrrg is Defectively Regulated in B6.*Sle1c2* $CD4^+$ T Cells

The 675Kb *Sle1c2* interval contains just 2 known genes, *Esrrg* and Usher syndrome 2A homolog (*Ush2a*) (Figure 2-1B), with the latter having no detectable expression in $CD4^+$ cells (data not shown). Contrary to *Ush2a*, *Esrrg* was detectable in $CD4^+$ splenocytes (Figure 2-6A). Furthermore, there was significantly less expression of *Esrrg* in $CD4^+$ (40.6±11.4% less, $p<0.001$), but not in $CD4^-$ splenocytes from B6.*Sle1c2* compared to B6. Like the $CD4^+$ T cell activation phenotype, there were no gender differences in *Esrrg* expression in age-matched mice of both strains. Regardless of age or strain, *Esrrg* expression showed a strong negative correlation with both $CD69^+$ and T_{em} percentages (Figure 2-6B), indicating a direct effect on $CD4^+$ T cells activation. These findings qualify *Esrrg* as the candidate gene for *Sle1c2*.

Since *Esrrg* coding sequence or UTR sequence differences were not found at the DNA level between the two strains, the causative allelic differences were predicted to lie in promoter or enhancer elements. As is the case for many nuclear receptors, *Esrrg* utilizes alternative promoters to encode transcripts with differing 5' UTR (Figure 2-1B) (138). While the promoters for this gene have not been thoroughly described, two of the transcripts have the same first exon (though they have slightly different transcript starts), and were thought to share a proximal promoter. The SNP that defines one end of the centromeric recombination interval of *Sle1c2*, rs31626695, lies at -156 and -197 relative to these two transcript start sites. However, an *in silico* analysis (139) did not define this region as a relevant transcription factor binding site, regardless of allele. Furthermore, it is outside of the highly conserved constrained element that

encompasses roughly 100bp of promoter and the entire first exon of these transcripts. Therefore, rs31626695 is likely not the causative allele. Sequencing from -450 to +1 revealed only 1 other allelic difference between the two strains. A missing adenosine in a series of 10 adenosines was found in NZW-derived *Sle1c2* at -260 relative to the beginning of transcript 1. Again, this area was not conserved and the missing adenosine is not predicted to affect transcription factor binding. A third transcript begins outside of the *Sle1c2* interval so there would not be genetic differences in that promoter (Figure 2-1B). Therefore, unless there are other unknown alternative promoters, as was the case for the murine paralog of *Esrrg*, Estrogen receptor 1 (alpha) (*Esr1*) (140), I theorized that the decreased *Esrrg* expression by *Sle1c2* is likely attributable to a polymorphism affecting an enhancer element. Deep sequencing of the *Sle1c2* locus is currently underway to reveal potential causative genetic differences.

Because *Esrrg* is known to be active in highly metabolic and in central nervous system tissues (141-144), cDNA from brain, heart, kidney, and liver from adult mice was examined to determine if *Sle1c2* resulted in differential regulation of *Esrrg* in these tissues as well. A trend for decreased expression was observed in kidney and liver, and in brain, *Esrrg* expression was significantly decreased (Figure 2-7C). Interestingly, an increased expression trend was observed in heart. *Esrrg*-deficient mice die postnatally due to a defective switch from glycolytic to oxidative metabolism (145). Consistent with *Esrrg*$^{-/-}$ mice, B6.*Sle1c2* mice also struggle to thrive and roughly three quarters of neonates die by day 2 (data not shown). It is possible that in response to failed *Esrrg* expression, a compensatory mechanism may allow for *Esrrg* to be upregulated in the myocardium of a small percentage of neonates, resulting in survival.

To determine if decreased expression of *Esrrg* in $CD4^+$ T cells had transcriptional consequences in its putative target genes, a set of genes that were differentially expressed by B6.*Sle1c* $CD4^+$ T cells in the gene expression analysis and were also known to have ERRγ bound to their promoters by chip-on-chip analysis (145, 146) were analyzed by quantitative RT-PCR. Five of the twelve genes analyzed had significantly decreased expression (Figure 2-7D). These included transcriptional regulators, c-myc binding protein (*Mycbp*) and retinoic acid receptor alpha (*Rara*), a subunit of electron transport complex I, NADH dehydrogenase (ubiquinone) Fe-S protein 1 (*Ndusf1*), a mitochondrial protein modifier, peptidylprolyl isomerase F (*Ppif*), and a mitochondrial oxidoreductase, reticulon 4 interacting protein 1 (*Rtn4ip1*). These data suggest that the decreased *Esrrg* expression induced by *Sle1c2* can affect *Esrrg* target gene expression. However, without evidence of ERRγ directly binding to control elements of these genes in $CD4^+$ cells, this data remains circumstantial.

The overall expression of *Esrrg* in $CD4^+$ T cells is low compared to other tissues. Liver had roughly 4 times, while kidney and brain had about 50 times the amount of *Esrrg* transcripts as $CD4^+$ T cells after normalizing to *Gapdh* (Figure 2-6C). Low message expression correlated with low protein expression, as ERRγ was not detectable by flow cytometry (data not shown). It was detectable by immunoblotting (Figure 2-6D), but the differences observed in mRNA expression could not be confirmed in the protein levels using this method. More sensitive techniques, such as ELISA, will need to be employed in order to assess *Sle1c2*'s ability to alter ERRγ levels in $CD4^+$ T cells.

It is unclear as to whether all $CD4^+$ T cells have a continuously ubiquitous low expression or if a small subpopulation expresses higher amounts of *Esrrg* under specific conditions. We attempted to clarify this question by checking the expression in FACS sorted naïve and T_{em} $CD4^+$ T cells. This sorting strategy was chosen because of the strong skewing effect that the *Sle1c2* locus has on these $CD4^+$ subpopulations. Our results showed that B6 T cells exhibit a strong upregulation in T_{em} cells as compared to naïve cells, while, in B6.*Sle1c2* mice, *Esrrg* expression remained constant in both populations (Figure 2-7B). However, this data is somewhat perplexing in that the naïve population in B6.*Sle1c2* had expression levels equal to the B6 T_{em} population. This would indicate an overall greater *Esrrg* expression in B6.*Sle1c2* $CD4^+$ T cells, which is contrary to our previous findings (Figure 2-6A).

Sle1c2 Exacerbates Lupus in the Induced cGVHD Model

For complex genetic diseases such as SLE to develop, epistatic interactions of multiple susceptibility alleles are required. When individual loci are isolated, as I have done with B6.*Sle1c2*, overt disease does not occur. In order to prove that the $CD4^+$ T cell phenotypes that segregated with *Sle1c2* are relevant to lupus pathogenesis, the cGVHD-induced lupus model was used (47, 147). This model was previously used to validate the larger *Sle1c* interval and preliminary mapping using subcongenic strains showed that increased cGVHD susceptibility mapped to the centromeric portion of the locus and so should be a phenotype of *Sle1c2* (52). This was in fact the case as B6.*Sle1c2* recipients of B6.bm12 adoptive transfers had significantly increased splenomegaly compared to B6 recipients (Figure 2-8A). In addition, their B cells were more activated and produced more autoantibodies (Figures 2-8B, 2-8C). Finally, the kidneys of B6.*Sle1c2* mice that had received B6.bm12 splenocytes showed an

increased deposition of pathogenic IgG2a immune complexes as compared to B6 recipients (Figure 2-8D).

The use of mixed bone marrow recipients showed that the *Sle1c2* induced ability of host B cells to be more responsive to cGVHD was actually intrinsic to T cells (Figure 2-8E). While this is consistent with our previous finding that *Sle1c2* is $CD4^+$ T cell intrinsic, the mechanisms governing *Sle1c2*-induced cGVHD sensitivity are not clear. The pathogenesis in this model has been reported to be mediated by alloreactive donor $CD4^+$ T and host B cell interactions (147). It has recently been reported, however, that host B cells require $CD4^+$ T cells during their ontogeny in order to be responsive to cGVHD (148). While there was clear evidence that IFNγ is dispensable for this process it is still plausible that increased production of IFNγ due to augmented T_H1 by *Sle1c2* can enhance B cell responsiveness to cGVHD or that it can directly enhance the cGVHD reaction. Alternatively, *Sle1c2* $CD4^+$ T cell hyperactivity may prime B cells for cGVHD through more generalized interactions, such as CD40 & CD40L (148).

Sle1c2 Mediates Severity of Spontaneous Lupus via Epistatic Interactions

To reconstitute the effect of epistasis, NZB x B6 F1 and NZB x B6.*Sle1c2* F1 hybrids were generated and aged to 12 months. In this model, which was previously used to validate the larger *Sle1c* interval (51), NZB susceptibility loci interact with either the NZW or the B6 alleles within the *Sle1c2* interval. Because this is an F1 model of spontaneous lupus, all loci are heterozygous, meaning there is only one copy of any given susceptibility allele, which would most likely be the case in human SLE. Our findings showed that splenomegaly, CD4:CD8 ratios, and T_{em} percentages were significantly increased when just 1 allele of the NZW derived *Sle1c2* was present (Figure 2-9A). Additionally, increased B7-2 expression in NZB x B6.*Sle1c2* mice

indicated that B cells were more activated as well (Figure 2-9A). Moreover, the addition of NZB loci allowed for B cells to generate pathogenic autoantibodies that increased with age (Figure 2-9B). This age-dependent increase was more pronounced when *Sle1c2* was present, and reflects the accumulation of activated $CD4^+$ T cells by *Sle1c2* in aged mice (Figures 2-2B, 2-3A 2-9A, 2-9B). Finally, GN was greatly exacerbated with the presence of *Sle1c2* (Figures 2-9C, 2-9D). Taken together, this data confirms *Sle1c2* as a pathogenic lupus susceptibility locus in spontaneous SLE.

Discussion

The major lupus susceptibility allele *Sle1* was originally described to consist of roughly 30% of telomeric Chromosome 1 (34). It was then reduced to the telomeric 20% of Chromosome 1 and determined to be NZW-derived when it was congenically transferred onto the lupus resistant B6 genome (149). Subsequent congenic dissection mapped *Sle1* associated $CD4^+$ T cell hyperactivation to *Sle1a* and *Sle1c* subloci (43, 50). The current study advances the work on *Sle1c*. Originally defined to be 7.72Mb, extending from D1MIT459 to the telomeric end of Chromosome 1, it contained 48 known protein coding genes and 4 known microRNAs. Previous analyses have shown that the phenotypic effect of this locus is due to at least two subloci, with *Cr2* established as the candidate gene for the telomeric *Sle1c1* sublocus (53), and an undefined gene regulating the centromeric *Sle1c2* sublocus (52). In this study, we have isolated *Sle1c2* as a single lupus susceptibility allele that enhances both induced and spontaneous models of murine lupus and associates with the previously observed $CD4^+$ T cell hyperactivation. Additionally, a strong T_H1 skewing, marked by a significant increase of IFNγ producing $CD4^+$ T cells, was found. Further, physical mapping and

gene expression analysis identified *Esrrg* as the candidate gene regulating this phenotype.

Dysregulated T cell activation is a major contributor to autoimmune diseases such as SLE and is therefore an important focus for therapeutic intervention (126, 150). One of the challenges of identifying newer more effective treatments has been in targeting specific T cell subsets. In this way, complications associated with the immunosuppression that occurs with more global targeting can be avoided. Even then, there is still the possibility that targeting some subsets may leave patients vulnerable to opportunistic infection. While the details of ERRγ's functional role in $CD4^+$ T cell biology is speculative at this point, this study suggests that pharmacological augmentation of its activity may alleviate pathogenic activation, effector memory accumulation, and T_H1 skewing.

Nuclear receptors are a family of transcription factors whose activities are mediated by binding of endogenous ligands and other coregulatory proteins. Several members of the nuclear receptor family have already been implicated in T cell biology, including retinoic acid receptor α (RARα), RAR-related orphan receptor γ (RORγ), vitamin D receptor, estrogen receptors, glucocorticoid receptor, and peroxisome proliferator-activated receptor-γ (PPARγ), (64, 151-153). ERRγ, belonging to the ERR family that also includes ERRα and ERRβ, does not yet have an established role in T cell biology. It is structurally related to the estrogen receptors, but does not bind natural estrogens (154, 155). In fact, endogenous ligands for ERRs have not been identified and they are thus referred to as orphan nuclear receptors. It has been shown, however, that ERRs are constitutively active due to properties of their ligand binding domains.

Therefore, their coregulatory proteins are considered to be the main mediators of their action (155). Regardless, several synthetic compounds have been shown to augment ERRγ-mediated transactivation of its target genes, demonstrating its potential as a therapeutic target (154). Interestingly, bisphenol A (BPA), an industrial component of some plastics and resins and known to be an endocrine disruptor, has been shown to bind to and alter the activity of ERRγ (156). This raises speculation that ERRγ may mediate environmental triggers of autoimmunity.

ERRs are important regulators of metabolism and energy homeostasis and *Esrrg* expression is highly restricted to metabolically active tissues (144, 154, 155). There, it transactivates genes involved in mitochondrial biogenesis, lipid transport and metabolism, tricarboxylic acid cycle, electron transport chain, and oxidative phosphorylation, allowing for energy production by efficient fatty acid oxidation. This vital function is demonstrated in *Esrrg* null mice, where the lack of a critical switch from glycolytic to lipid based metabolism in the myocardium results in perinatal lethality (145). Activation and proliferation by T cells is also metabolically demanding (157). However, contrary to other metabolically demanding tissues, activated T cells employ aerobic glycolysis to meet energy requirements. Known as the Warberg effect, this form of metabolism generates glucose metabolites at the expense of ATP production. This is advantageous to proliferating cells where substrate for biosynthesis, not ATP, is the limiting component (158). Remarkably, enhancement of the Warburg effect may result in T cell hyperactivation, as evidenced by mice with enhanced ability to sequester glucose. A report using mice that are transgenic for the T cell glucose transporter, glucose transporter type 1 (GLUT1), or that have enhanced ability to traffic GLUT1 to

the cell surface, found T cell hyperactivation phenotypes very similar to B6.*Sle1c2* mice, namely, age-dependent accumulation of $CD69^+$ and T_{em} cells, increased proliferation, and increased IFNγ production (159). Consequently, aged mice suffered from hypergammaglobulinemia and GN, exhibiting a direct connection between energy metabolism and autoimmunity. A more recent report demonstrated how T_H1, T_H2, and T_H17 lineage commitment requires glycolytic metabolism and is suppressed by fatty acid oxidation, while T_{reg} differentiation requires lipid metabolism (160). *Sle1c2* may similarly contribute to the Warberg effect in $CD4^+$ T cells as decreased *Esrrg* expression would limit transcription of target genes that regulate oxidative lipid based metabolism, skewing toward glucose based programs. ERRγ is therefore an attractive target for novel therapies.

Table 2-1. ERRγ Target Genes

Gene ID	Gene Name	Forward primer	Reverse primer	Reference
As3mt	arsenic (+3 oxidation state) methyltransferase	CCAGGGCCGTTCTGAGTT	TGTCCTTTAGCCACCCTCTTG	(146)
Cd59a	CD59a antigen	CTCATCTTACTCCTGCTGCTTCT	CCAACACCTTTGATACACTTGC	(146)
Crtam	cytotoxic and regulatory T cell molecule	CATCATCGTTCAGCTCTTCATC	TGGGCACTCTTCTTTGTTTTG	(146)
Esrra	estrogen related receptor, alpha	CTGAAAGCTCTGGCCCTTG	CTGTCTGGCGGAGGAGTG	(161)
Fabp4	fatty acid binding protein 4, adipocyte	GAAATCACCGCAGACGACA	TTCATAACACATTCCACCACCA	(145)
Mycbp	c-myc binding protein	GCTGGACACGCTGACGAA	TCTGGGTTTTCCGGGGTAG	(146)
Ndufs1	NADH dehydrogenase (ubiquinone) Fe-S protein 1	TGACCCACTCGTTCCACCT	CGGCTCCTCTACTGCCTGA	(146)
Ppargc1a	peroxisome proliferative activated receptor, gamma, coactivator 1 alpha	TACGCAGGTCGAACGAAAC	GTGGAAGCAGGGTCAAAATC	(162)
Ppif	peptidylprolyl isomerase F (cyclophilin F)	CGTGGTGCTGGAGTTAAAGG	CTGTGCCATTGTGGTTGGT	(146)
Rara	retinoic acid receptor, alpha	TCCCCAAGATGCTGATGAA	CCCGACTGTCCGCTTAGA	(146)
Rtn4ip1	reticulon 4 interacting protein 1	AGAACTGGTGGATGCAGGAA	GGGAGAATGTGTGGTGAAGG	(146)
Steap3	STEAP family member 3	CCCGTCCATTGCTAATTCC	GTCCAGCCGTAGGTGAGTGT	(146)

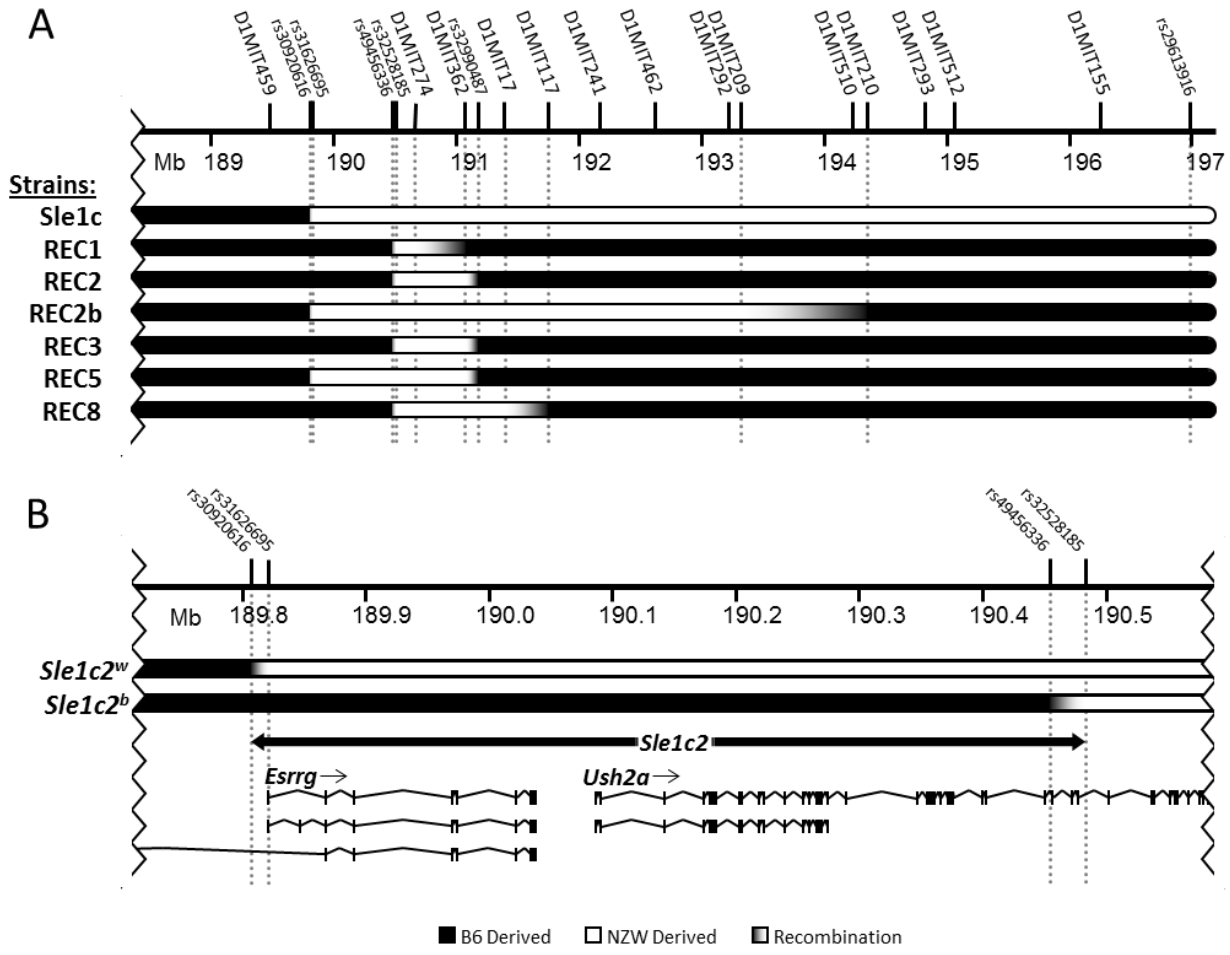

Figure 2-1. Physical map of the *Sle1c* locus. The intervals for *Sle1c* and its subcongenics are shown in (A), while *Sle1c2* along with the exon-intron structures for its two known protein coding genes are shown in (B). NZW derived regions are white and B6 derived regions are black. All known polymorphic MIT microsatellite markers, as well as SNPs that define recombination intervals are depicted. Scale is in Mb and all positions are current with Ensemble release 67 (www.ensembl.org/Mus_musculus/), which is based on NCBI m37.

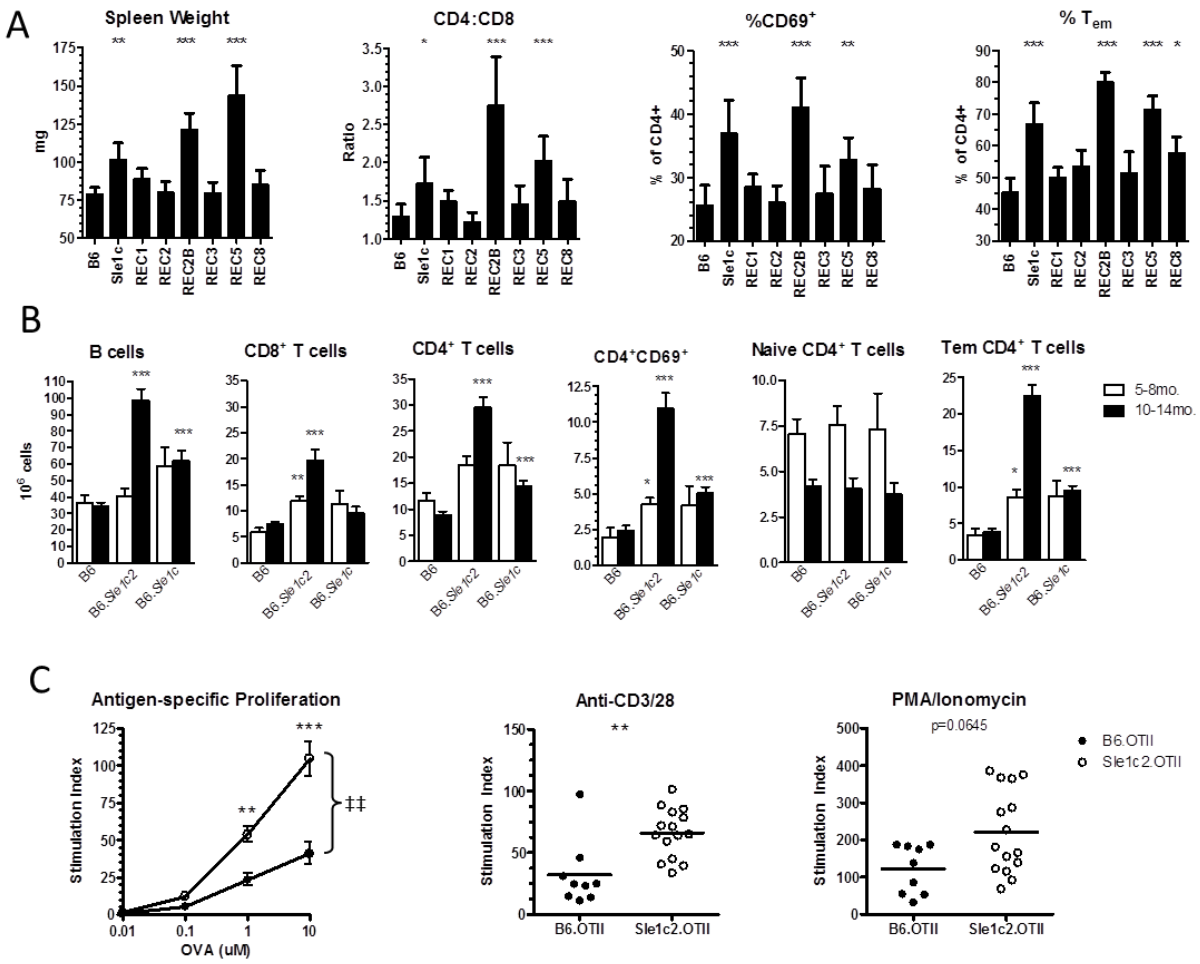

Figure 2-2. Mapping phenotypes used to define *Sle1c2*. Strain comparison of spleen weights and $CD4^+$ T cell activation determined by flow cytometry of splenocytes from 10-14 month old mice (A). Total cell numbers of B and T cell compartments were obtained from FACS analyses of splenocytes from 5-8 month old and 10-14 month old mice grouped by locus (B). Naïve T cells are defined as $CD4^+CD44^{lo}CD62L^+$ and T_{em} cells are defined as $CD4^+CD44^{hi}CD62L^-$. Antigen-specific and polyclonal proliferation of $CD4^+$ T cells was measured by ^3H thymidine incorporation (C). REC2B and REC5 subcongenic strains and REC2B.OTII and REC5.OTII bicongenic strains were used as *Sle1c2* and *Sle1c2*.OTII respectively. Significance in (A) indicates Dunn's multiple comparison analysis to B6. Significance in (B) indicates Mann-Whitney comparison to B6 of the same age group. Two-way ANOVA was used to measure strain effect on antigen-specific proliferation with Bonferroni's posttest indicating significance at each concentration (C). Student's *t*-test was used to compare polyclonal and mitogen-induced proliferation to B6 (C). * $P \leq 0.05$, ** $P \leq 0.01$, *** $P \leq 0.001$, ‡‡ $P \leq 0.001$

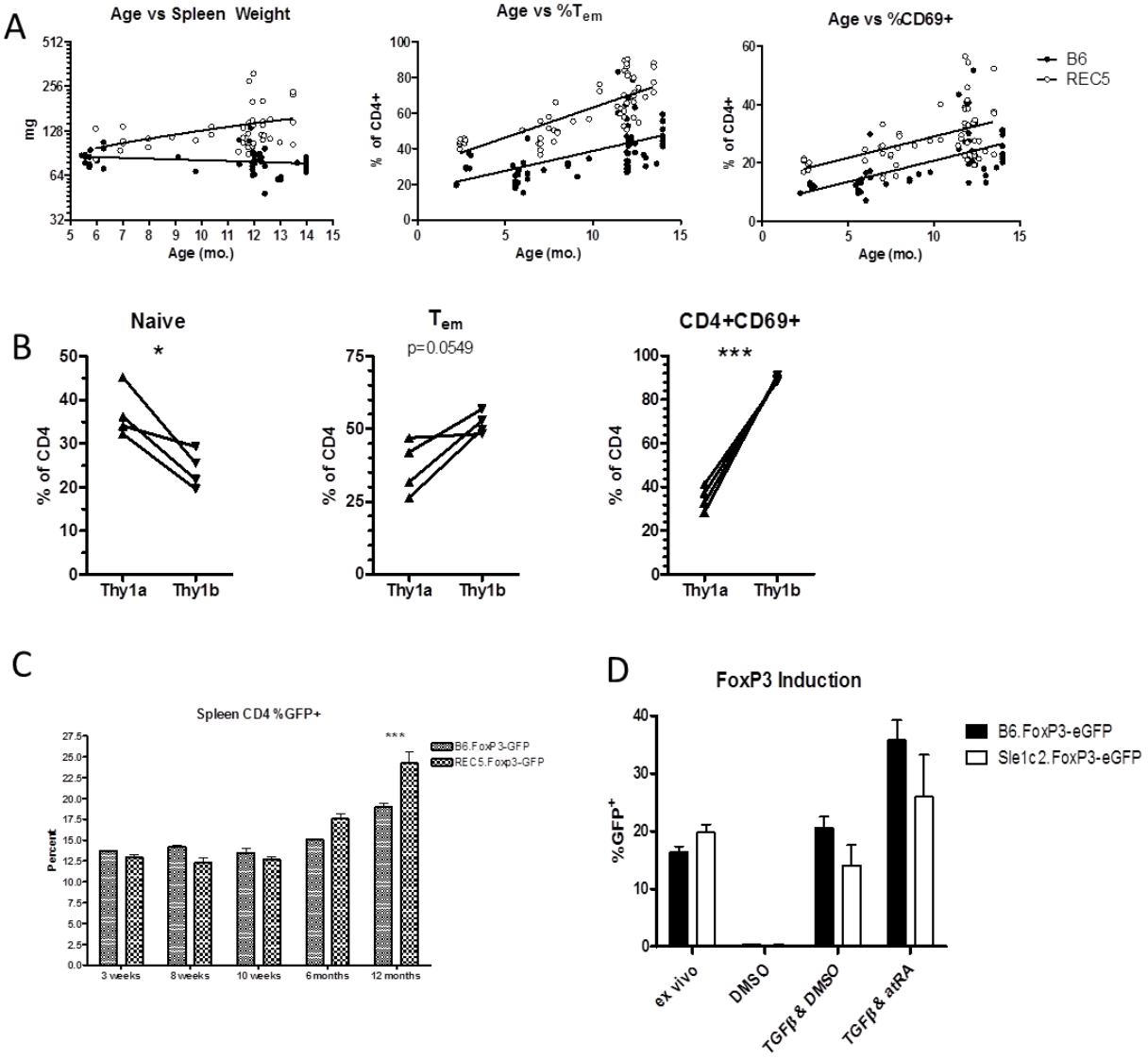

Figure 2-3. Additional *Sle1c2* phenotypes. Comparison of B6 and *Sle1c* subcongenic REC5 spleen weights and $CD4^+$ T cell activation over time as determined by flow cytometry (A). FACS analysis of B6.Thy1a and B6.*Sle1c2* (Thy1b) mixed bone marrow chimeras (B). GFP^+ percentages of $CD4^+$ T cells from B6.FoxP3-eGFP and B6.*Sle1c2*.FoxP3-eGFP was measured over the lifetime (C). GFP^+ percentages from B6.FoxP3-eGFP and B6.*Sle1c2*.FoxP3-eGFP were measured by flow cytometry both *ex vivo* and after *in vitro* induction of FACS sorted $CD4^+FoxP3^-$ T cells under T_H0 (anti-CD3 and -CD28 only), and T_{reg} (with TGFβ and with or without atRA) polarizing conditions. Student's *t*-tests were used in (B) and Bonferroni's multiple comparison was used in (C). * $P \leq 0.05$, ** $P \leq 0.01$, *** $P \leq 0.001$.

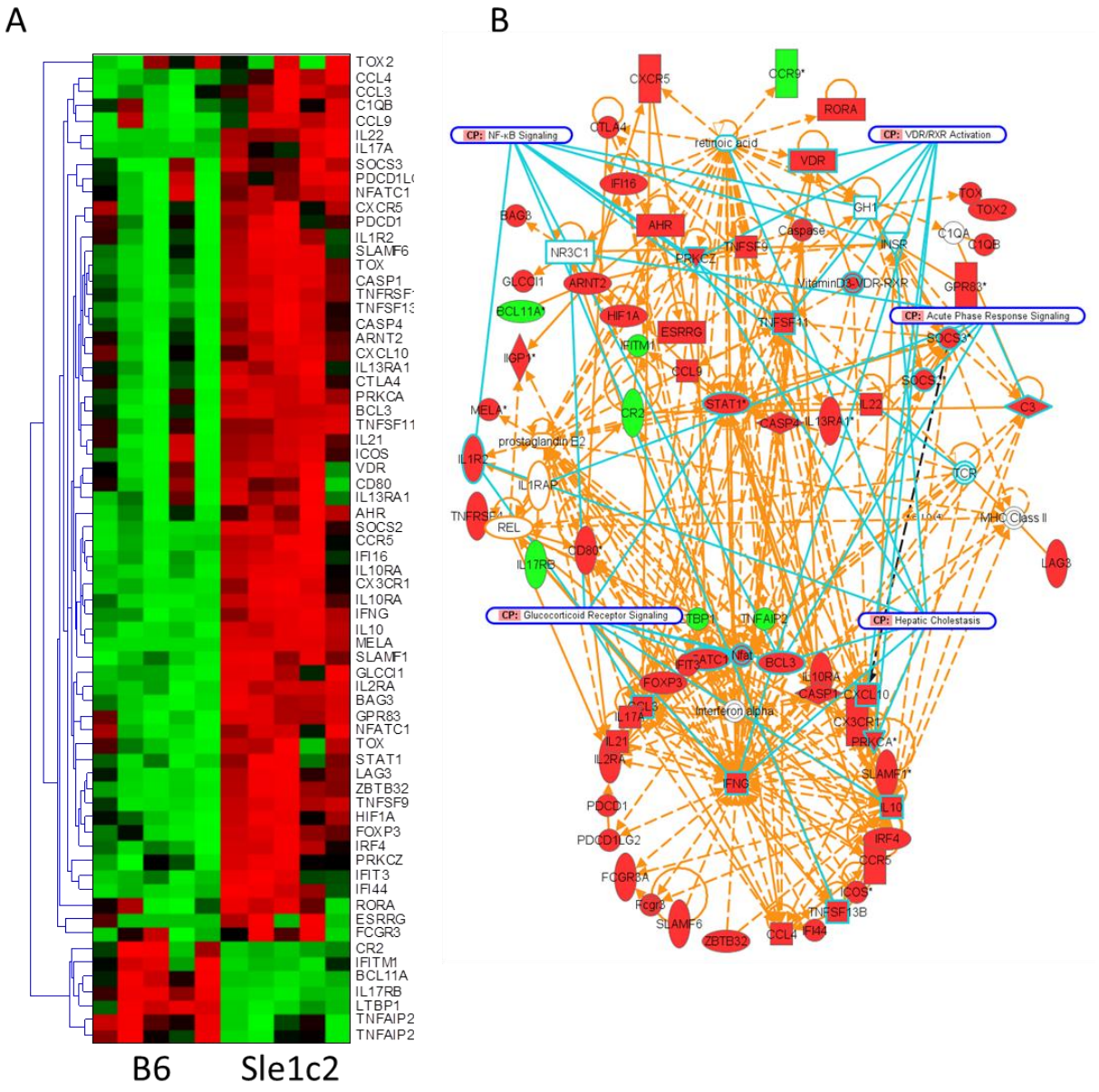

Figure 2-4. Global gene expression of CD4^{+} T cells. Heat map (A) and pathway analysis (B) of genes related to *Ifng* expression.

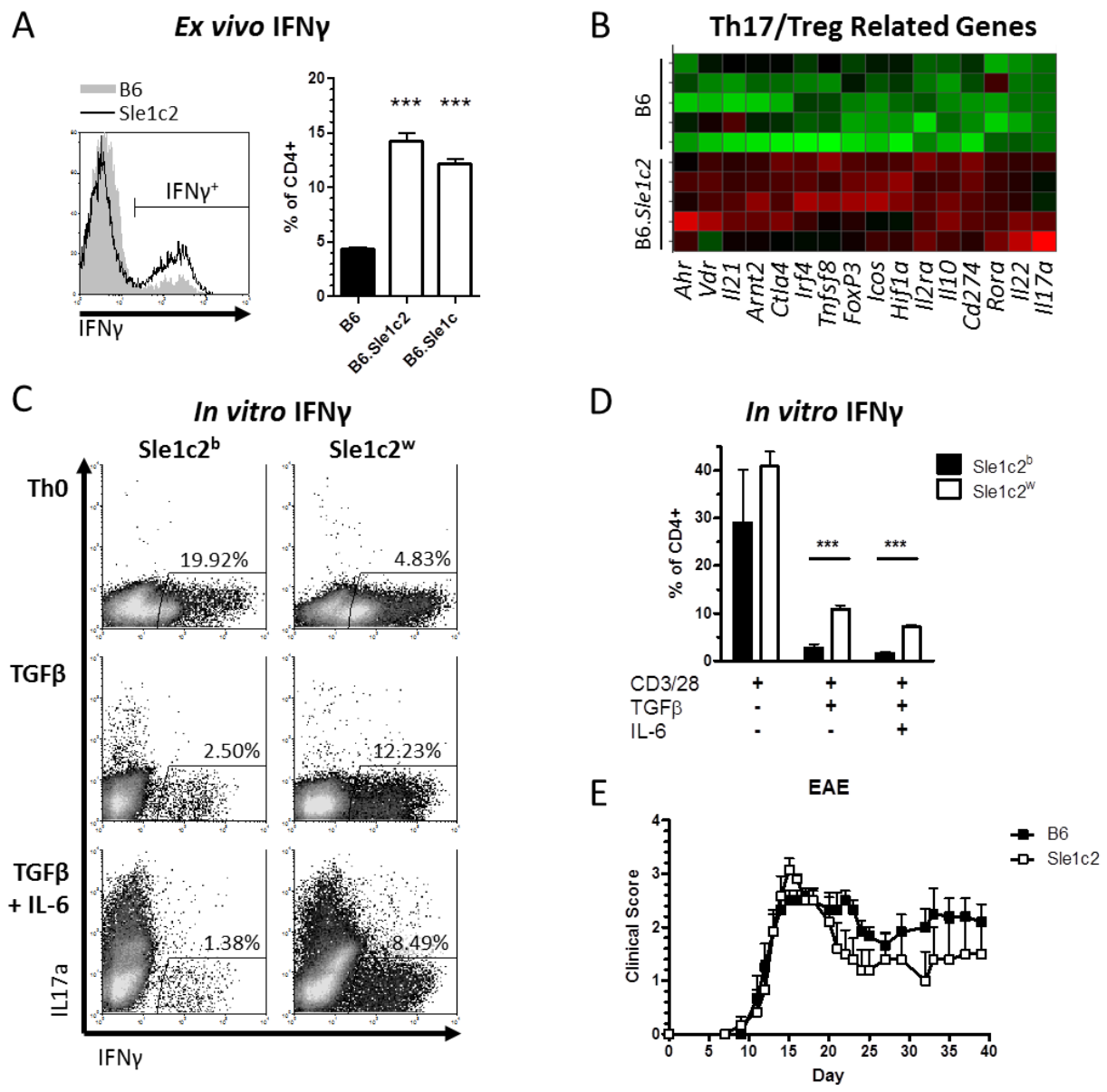

Figure 2-5. *Sle1c2* generates augmented T_H1 lineage. Representative histograms and quantification of intracellular staining for IFNγ in $CD4^+$ T cells were from 2-3 month old mice (A). A heat map illustrates upregulated expression of genes involved in T_H17 and T_{reg} homeostasis by B6.*Slec2* $CD4^+$ T cells (B). Representative plots of intracellular staining (C) and quantification (D) shows increased IFNγ production by B6.*Slec2* $CD4^+$ T cells cultured under T_H0 (anti-CD3 and -CD28 only), T_{reg} (with TGFβ), and T_H17 (with TGFβ and IL-6) polarizing conditions. EAE clinical scores did not significantly differ between B6 and B6.*Sle1c2* (n=6) (E). Student's *t*-test: * $P \leq 0.05$, ** $P \leq 0.01$, *** $P \leq 0.001$.

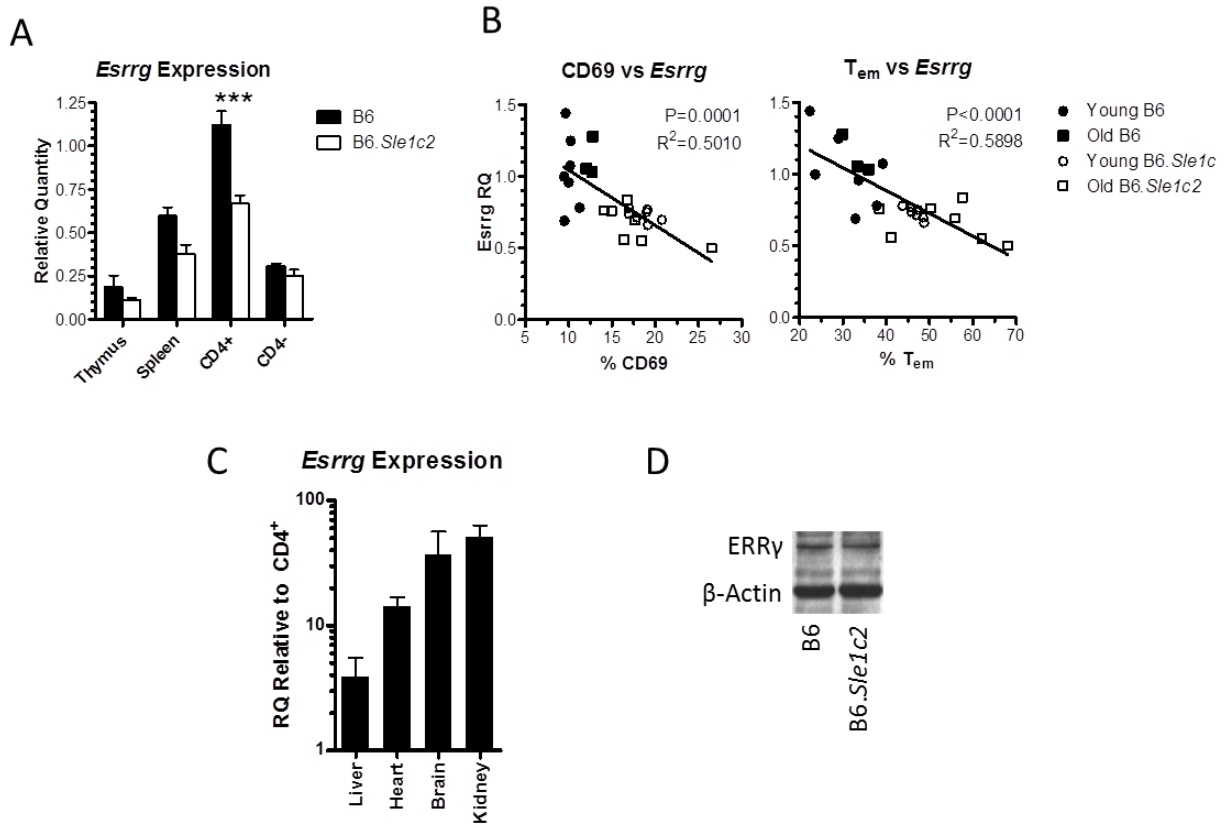

Figure 2-6. *Sle1c2* results in decreased expression of *Esrrg* by $CD4^+$ T cells. qPCR comparing *Esrrg* expression from thymocytes, splenocytes, $CD4^+$ T cells, and non-$CD4^+$ T cell fraction ($CD4^-$) between B6 and B6.*Sle1c2* (A). Correlation between *Esrrg* expression by $CD4^+$ T cells and $CD69^+$ and T_{em} percentages of CD4 (B). *Esrrg* expression in various tissues by B6 mice, normalized to *Gapgh* and relative to B6 $CD4^+$ T cell expression (C). Western Blot of ERRγ and Actin (D). Student's *t*-tests were used to compare *Esrrg* expression to B6 for each cell population in (A). Significance that slope does not equal zero (P) and correlation coefficient for linear regressions (R^2) are shown in (B). *** $P \leq 0.001$

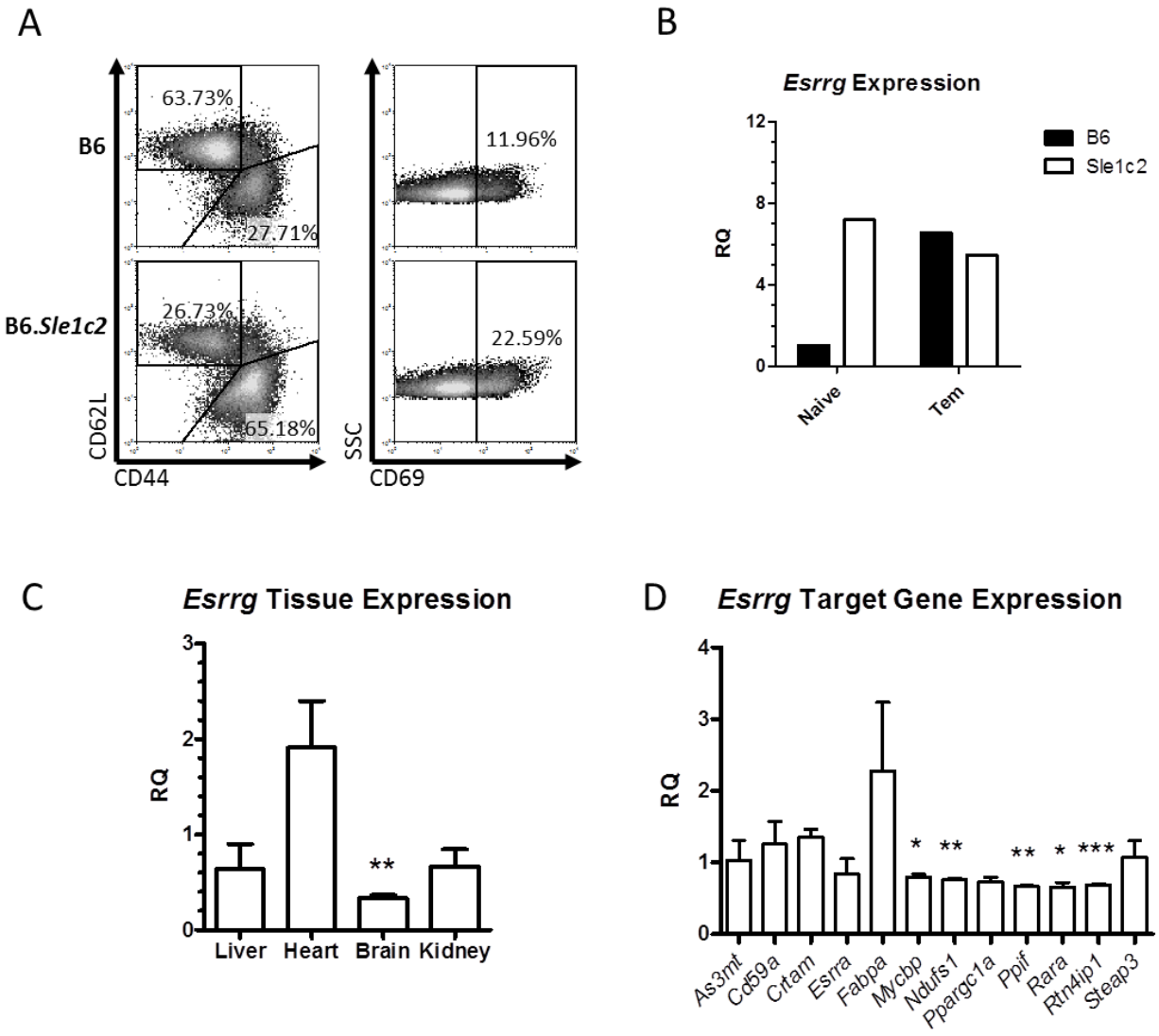

Figure 2-7. Additional *Esrrg* expression data. Representative FACS plots of $CD69^{+}$ and T_{em} ($CD44^{hi}CD62L^{-}$) used to analyze correlation to *Esrrg* expression in Figure 2-6B (A). *Esrrg* expression of FACS sorted Naïve ($CD4^{+}CD44^{lo}CD62L^{+}$) and T_{em} ($CD4^{+}CD44^{hi}CD62L^{-}$) cells from B6 and B6.*Sle1c2* splenocytes (B). *Esrrg* expression in various tissues by B6.*Sle1c2* mice, normalized to *Gapgh* and relative to the B6 expression in that same tissue (C). Expression of various genes reported to be regulated by ERRγ, normalized to *Gapdh* and relative to the B6 expression of that same gene (D). Student's *t*-test: * $P \leq 0.05$, ** $P \leq 0.01$, *** $P \leq 0.001$.

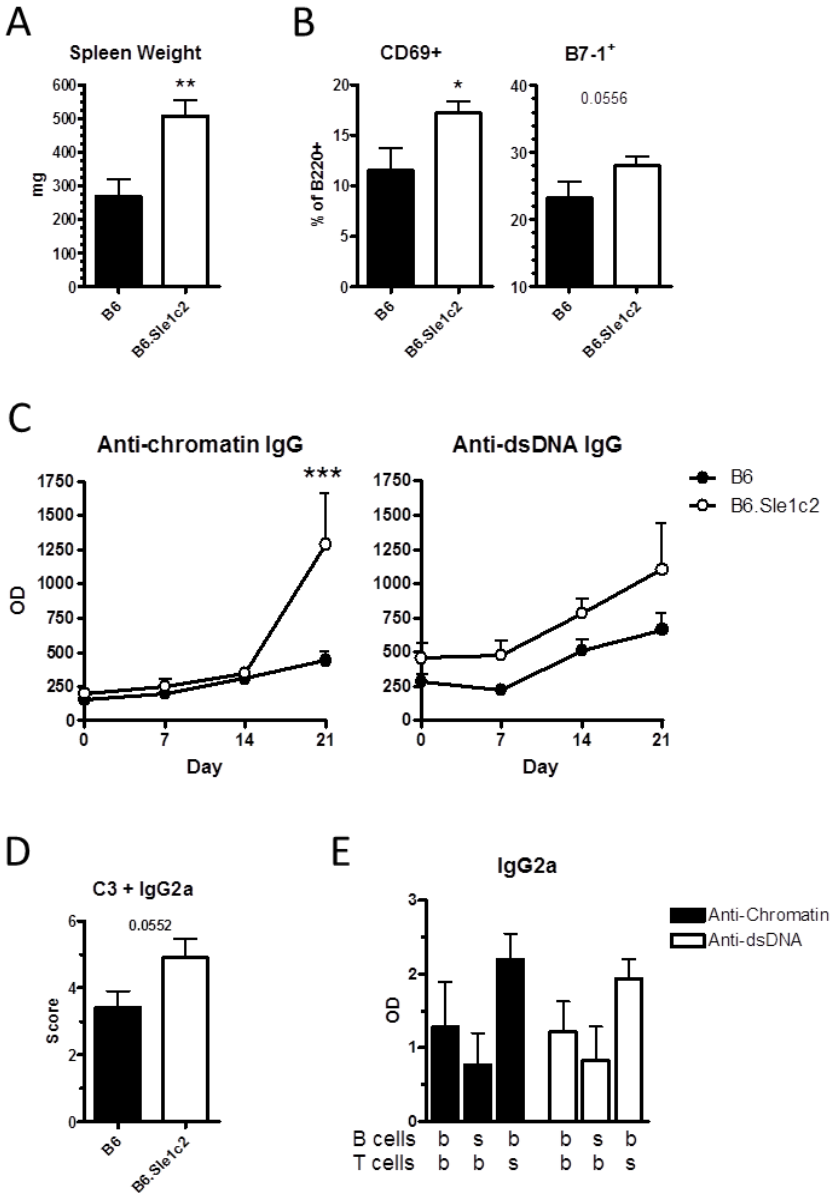

Figure 2-8. Sle1c2 exacerbates induced lupus in a T cell intrinsic manner. cGVHD was induced in B6 and B6.Sle1c2 mice and spleens were weighed (A) and B cell activation was measured by FACS (B) after 3 weeks. Sera were collected once a week, beginning a day 0, and anti-dsDNA and anti-chromatin IgG were measured by ELISA (C). IgG2a and C3 deposition was detected in frozen kidney sections (D). Sections were separately scored in a blind manner and additive values are shown. cGVHD was also induced in mixed bone marrow chimeras such that B and T cells were either of B6 (b) or B6.Sle1c2 (s) origin and autoantibodies were measured at 5 weeks (E). Student's *t*-test was used to compare to B6 in (A), (B), (D), and (E). Bonferroni's multiple comparison was used in (C). * $P \leq 0.05$, ** $P \leq 0.01$, *** $P \leq 0.001$

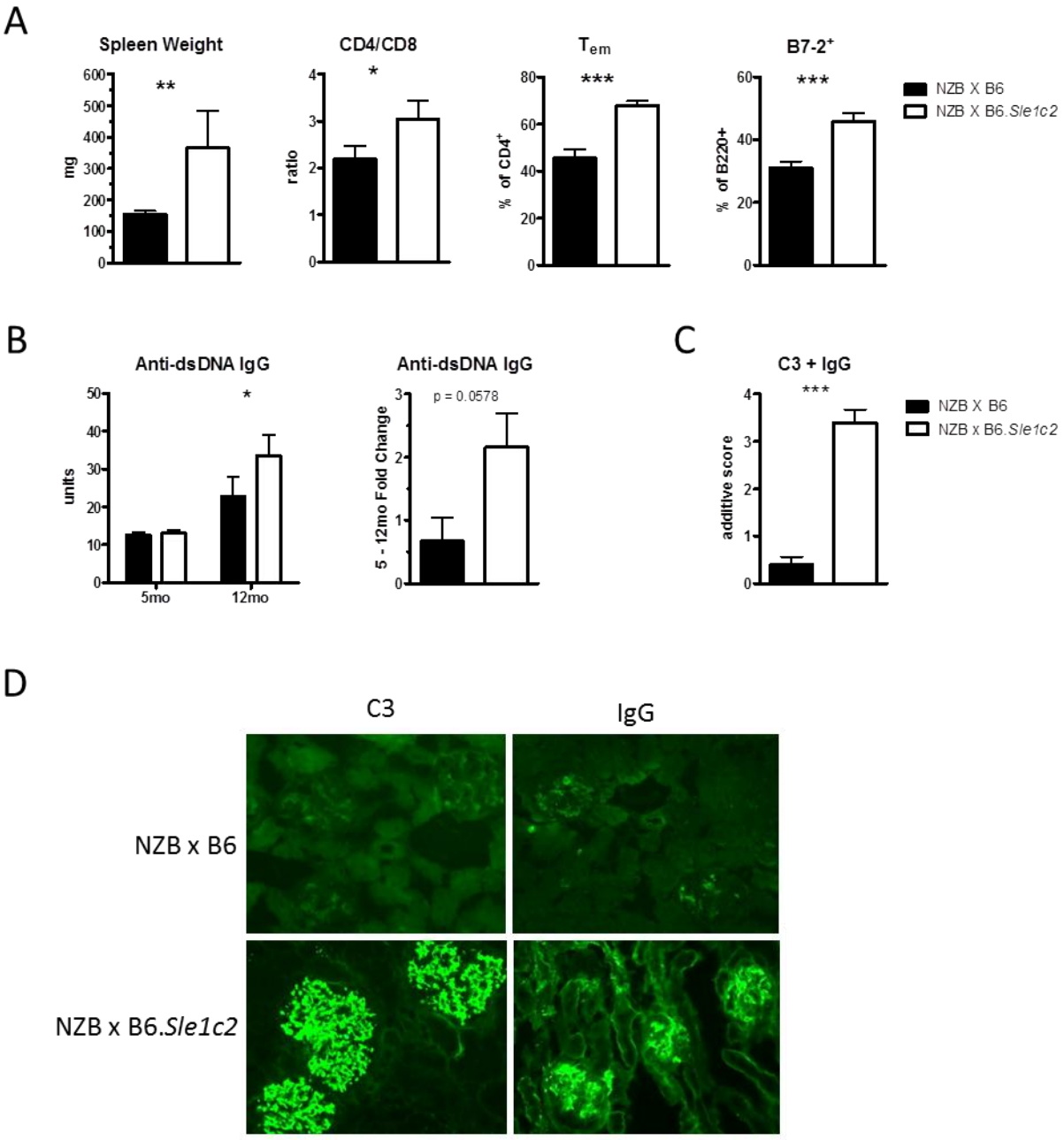

Figure 2-9. *Sle1c2* exacerbates spontaneous lupus. Spleen weight and flow cytometry data were quantified from 12 month old NZB x B6 F1 and NZB x B6.*Sle1c2* F1 mice (A). Anti-dsDNA IgG was measured at 5 and 12 months (B). IgG and C3 deposition was detected in frozen kidney sections (C, D). Sections scored in a blind manner and additive values are shown. Student's *t*-test was used to compare to NZB x B6. * $P \leq 0.05$, ** $P \leq 0.01$, *** $P \leq 0.001$

CHAPTER 3
DISCUSSION

Sle1c2 has been pared down to 675Kb from the 7.5Mb *Sle1c* interval. We have shown that this region is sufficient to confer the $CD4^+$ T cell hyperactivation that was originally observed in B6.*Sle1c* mice. Mixed bone marrow chimeras showed that this was $CD4^+$ T cell intrinsic. Further, a prominent T_H1 skewing was found as B6.*Sle1c2* mice had significantly more IFNγ producing $CD4^+$ cells that B6 mice. Additionally, the ability to exacerbate both spontaneous and induced lupus segregated with *Sle1c2*. The use of FoxP3-eGFP knock-in mice indicated that, contrary to previous reports (52), T_{reg} were not decreased in *Sle1c2* mice. This last finding is likely due to the fact that the previous reports defined T_{regs} by surface phenotype $CD4^+CD25^+CD62L^+$, not by expression of the master regulator FoxP3, which is a more accurate way to measure T_{regs} (59, 134). The major accumulation of T_{EM} cells, which are $CD62L^-$, was likely the reason that T_{regs} appeared less frequent when measuring by surface phenotype.

The fine mapping of *Sle1c2* has allowed for a considerable reduction of positional candidate genes from 48 to 2. Of these, only *Esrrg* was expressed in $CD4^+$ T cells. Expression in the $CD4^+$ cell compartment is essential to qualify as a candidate because the*Sle1c2* phenotype is $CD4^+$ T cell intrinsic. No coding sequence or isoform differences were found between the NZW and B6 derived alleles if *Esrrg*. There was, however, a decreased expression in *Sle1c2* splenocytes that segregated with $CD4^+$ T cells. Most compellingly, *Esrrg* expression had a very strong negative correlation with $CD4^+$ T cell activation phenotypes.

ERRγ, along with ERRα and ERRβ, belong to a family of orphan nuclear receptors that are closely related to estrogen receptors, but do not bind natural estrogens (163).

They mediate transcription of their target genes by binding to estrogen response elements (AGGTCAnnnTGACCT) either as homodimers or heterodimers and to modified half sites, known as ERR-response elements (TnAAGGTCA) as monomers (163). Their endogenous ligands are not known, but it has been shown that they have a fairly high level of constitutive activation (164). The action on target genes is therefore mediated by the concentration of coactivators, such as peroxisome proliferator-activated receptor γ-coactivator 1α (PGC-1α) and corepressors, such as receptor-interacting protein 140 (RIP140) (165, 166). Synthetic ligands with differing activities on ERRs have been identified, allowing for pharmacological stimulation or inhibition. GSK4716 shows selective agonist activity, while 4-Hydroxytamoxifen (4-OHT) works as an inverse agonist (167, 168). A preliminary *in vitro* culture of $CD4^+$ T cells with GSK4716 or 4-OHT did not find differences in CD44, CD69, or IFNγ (data not shown). There was suggestive data for an opposing dose-response effect of these agents on CD62L such that 4-OHT increased, and GSK4716 decreased expression. This may be a promising result, but would need to be repeated with estrogen to control for the effect 4-OHT has on estrogen receptors.

As was covered in the discussion of the last chapter, ERRγ has a vital role in the regulation of oxidative metabolism (154). Evidence that energy metabolism can regulate T cell homeostasis is growing and would be a subject to explore in *Sle1c2* $CD4^+$ T cells (157). The work done by the Rathmell group is especially intriguing in that it provides a direct explanation of how less ERRγ would skew T cell metabolism toward a glycolytic program that allows for an expansion of T_H1 subsets (159, 160). To

evaluate this hypothesis, glycolysis and lipid oxidation rates of B6.*Sle1c2* $CD4^+$ T cells should be measured as they were by Rathmell et al. (160).

An important aspect of this project that requires clarification is whether the protein levels of ERRγ reflect the same decrease seen by RNA expression. Since the coding sequence in the NZW allele is identical to the B6 allele and splice isoforms have not been found (data not shown), post-transcriptional and post-translational modifications and regulation are predicted to also be unaltered. However, several attempts at semi-quantitative assessment of ERRγ levels by western blotting have failed to show a difference. It is likely that this method is not sensitive enough. As discussed in the last chapter, expression and protein levels of are very low, requiring a large amount (at least 50µg) of total protein to be loaded for SDS-PAGE, which may obscure any subtle differences. A more sensitive ELISA should be attempted.

One of the initial goals of this project was to replicate the effect of *Sle1c2*, either by decreasing expression of *Esrrg* in B6 $CD4^+$ T cells or by increasing it in B6.*Sle1c2* $CD4^+$ T cells. An expression vector was constructed that expressed *Esrrg* with a GFP reporter (Appendix B). The construct works as expected in 293 cells. However, we are so far unable to transfect primary $CD4^+$ T cells, as the cells don't survive the transfection process. The future plan is to subclone this construct into a lentiviral vector. This should lead to higher viability and more stable expression so that the effect of ERRγ can be addressed *in vivo*. Additionally, pre-manufactured lentivirus expressing *Esrrg*-specific shRNA (Openbiosystems) will be used to recapitulate *Sle1c2* decreased *Esrrg* expression *in vivo*. Ultimately, endogenous *Esrrg* can be conditionally deleted or knocked down in the $CD4^+$ T cells of B6 mice. This can be done by crossing mice

expressing a CD4-*Cre* transgene to mice with either a floxed *Esrrg* locus or to mice with an *Esrrg*-specific shRNA inserted downstream of a Rosa26-Stop$^{fl/fl}$ locus. B6 mice containing the CD4-*Cre* transgene and the Rosa26-Stop$^{fl/fl}$ locus are available from the Jackson Laboratories. The floxed *Esrrg* locus and *Esrrg*-specific shRNA knocked into the Rosa26-Stop$^{fl/fl}$ locus would have to be generated.

Finally, ChIP-Seq will reveal novel insights into transcriptional programs that are regulated by ERRγ in CD4$^+$ T cells. I predict that ERRγ will be found to bind to regulatory elements of genes involved in oxidative metabolism, as has previously been found in other tissues (141-144). Coupled with differential metabolic functional findings (discussed above), a novel role for ERRγ in the metabolic control of CD4$^+$ T cell function will be established. There may also be other gene programs that are regulated by ERRγ in CD4$^+$ T cells which may result in the *Sle1c2*-induced hyperactivation and T_H1 skewing of CD4$^+$ T cells. As there is currently no description of ERRγ in T cells, the insights gained from these experiments will elucidate novel pathways whose dysregulation can mediate autoimmunity.

APPENDIX A
IN SILICO IDENTIFICATION OF POTENTIAL CAUSITIVE *SLE1C2* ALLELES RESPONSIBLE FOR *ESRRG* DOWNREGULATION

An *in silico* analysis was performed in an effort to narrow the set of total polymorphic SNPs to a smaller set that are more likely to affect transcription or *Esrrg.* A set SNPs that are polymorphic between B6 and NZB was selected based on their position within constrained elements for 35 eutherian mammals (www.ensembl.org). Where the NZW allele was not available, the DBA allele was assumed based on the high sequence homology between the two strains in the *Sle1c2* region (Figure A-1). This produced a set of 21 SNPs that were used to perform an *in silico* analysis for differential transcription factor binding (139) (Table A-1). The analysis yielded a few intriguing data (Table A-2). First, the NZW allele of rs32271729 removes a Pbx1 binding site. As this is the candidate gene for *Sle1a1*, a potential explanation for epistatic interaction between *Sle1a1* and *Sle1c2* is revealed. Second, the NZW allele of rs31811886 removes a PPAR:RXR site. Like ERRγ, peroxisome proliferator-activated receptors (PPARs) and the retinoid X receptors (RXRs) are known to play a role in energy homeostasis (169). Therefore, this SNP could represent a disconnect from a metabolic transcriptional program. Finally, the NZW allele of rs32038280 removes an highly conserved (Figure A-2) interferon regulatory factor 1 (IRF-1) site and adds a HNF1 homeobox A (HNF1a) site. This may tie into the T_H1 skewing such that IFNγ signaling may activate *Esrrg* through IRF1, which would activate lipid oxidation programs that would negate the oxidative glycolysis that is essential for efficient T_H1 differentiation. The NZW allele would lack this negative feedback loop.

This analysis is based on some assumptions that aren't necessarily true. First, the causative allele may not be a SNP. It may be an indel or some other structural variant,

or it may be a novel SNP that would not be annotated. Second, the causative allele may not be in a constrained region. Third, the decreased expression of *Esrrg* may be due to more than one polymorphism. Regardless of these assumptions, this analysis sets a logical starting point for uncovering the genetic cause for decreased *Esrrg* by *Sle1c2*.

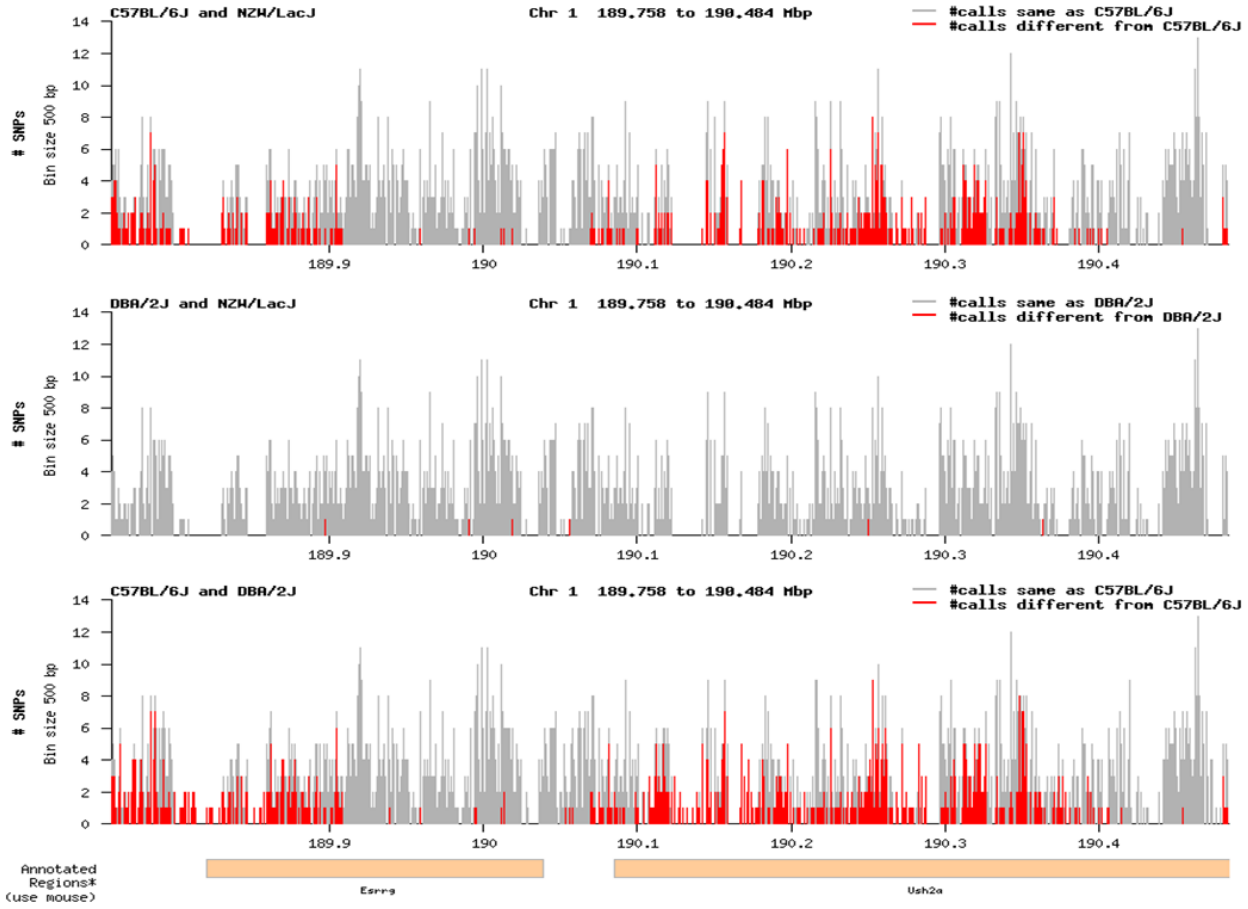

Figure A-1. Comparative SNP analysis of *Sle1c2*. B6 vs NZW (Top); DBA vs NZW (Middle); B6 vs DBA (Bottom)

Table A-1. SNPs in constrained elements

SNP	Position (Chr:Mb)	B	D	W	Constrained Element	Length (bp)	Score	p-value
rs32278316	1:189819821	G	A	nd	1:189819730-189820148	419	688.60	1.94e-23
rs32524022	1:189837554	C	T	T	1:189837499-189837723	225	434.40	6.29e-21
rs31690177	1:189854244	C	T	nd	1:189853716-189854496	781	1766.40	3.36e-144
rs32271729	1:189857580	T	C	nd	1:189857321-189857741	421	559.70	2.94e-31
rs32099068	1:189857612	A	G	nd	1:189857321-189857741	421	559.70	2.94e-31
rs31811886	1:189858530	T	C	C	1:189858361-189858686	326	867.30	7.20e-84
rs32239074	1:189860163	G	C	C	1:189859871-189860209	339	1209.00	6.12e-184
rs32038280	1:189865403	G	A	A	1:189865266-189865590	325	1035.70	1.96e-125
rs3667534	1:189866887	T	C	C	1:189866872-189867047	176	441.80	4.54e-45
rs31081923	1:189881827	A	G	G	1:189881778-189881982	205	417.40	1.93e-35
rs31690423	1:189884459	C	A	nd	1:189884317-189884608	292	911.50	2.34e-115
rs30473053	1:189885064	G	C	C	1:189884976-189885373	398	569.80	1.39e-32
rs3673367	1:189886643	G	A	A	1:189886617-189886768	152	201.10	1.06e-12
rs3683961	1:189903263	G	A	A	1:189903149-189903299	151	152.80	5.03e-08
rs32085863	1:189903441	T	G	nd	1:189903362-189903484	123	141.70	9.11e-09
rs2228901	1:189905663	T	C	C	1:189905588-189905760	173	499.70	7.37e-58
rs30572892	1:189906487	C	A	A	1:189906364-189906546	183	500.80	4.55e-57
rs31400926	1:189906947	T	A	A	1:189906836-189907224	398	1402.60	2.36e-212
rs32757999	1:189907183	T	C	C	1:189906836-189907224	398	1402.60	2.36e-212
rs30993521	1:190011782	G	A	A	1:190011495-190012021	527	921.90	9.19e-65
rs3694567	1:190013851	G	C	C	1:190013798-190013848	51	78.70	1.40e-06

Table A-2. SNP effects on transcription factor binding

Sequence	Position	Model	Factor	Strand	B6 Score	NZW Score	Change
rs32278316	1:189819821	T01471	Ik-3	+	-	2.6	2.60
rs32278316	1:189819821	M00059	YY1	-	2.5	-	2.50
rs32278316	1:189819821	M00706	TFII-I	+	-	2	2.00
rs32524022	1:189837554	M00162	1-Oct	+	-	2.7	2.70
rs32524022	1:189837554	M00238	Barbie Box	-	3.4	4.5	1.10
rs31690177	1:189854244	M00480	LUN-1	+	2.8	-	2.80
rs31690177	1:189854244	MA0028	ELK1	-	2	-	2.00
rs31690177	1:189854244	T04446	Nkx5-1	-	6.1	4.4	1.70
rs31690177	1:189854244	MA0026	Eip74EF	-	1.6	-	1.60
rs32271729	1:189857580	M00124	Pbx-1b	-	5.2	-	5.20
rs32271729	1:189857580	T05671	NIL	-	5	-	5.00
rs32271729	1:189857580	MA0070	PBX1	-	3.4	0.8	2.60
rs32271729	1:189857580	MA0041	Foxd3	-	2	-	2.00
rs32271729	1:189857580	MA0017	NR2F1	-	1.7	-	1.70
rs32099068	1:189857612	M00026	RSRFC4	-	4.3	-	4.30
rs32099068	1:189857612	T00422	IRF-1	-	4	-	4.00
rs32099068	1:189857612	M00408	MADS-A	+	2.7	-	2.70
rs32099068	1:189857612	MA0038	Gfi	-	0.7	1.9	1.20
rs31811886	1:189858530	M00242	PPARalpha:RXRalpha	+	4.4	-	4.40
rs31811886	1:189858530	M00415	AREB6	-	-	2.8	2.80
rs31811886	1:189858530	T00772	STE12	-	-	2.2	2.20
rs31811886	1:189858530	MA0072	RORA_2	+	2.1	-	2.10
rs31811886	1:189858530	M00664	STE12	+	-	2	2.00
rs31811886	1:189858530	MA0071	RORA_1	+	1.4	-	1.40
rs31811886	1:189858530	MA0011	br_Z2	-	1.1	-	1.10
rs31811886	1:189858530	MA0045	HMG-I/Y	+	-	1	1.00
rs32239074	1:189860163	M00681	WRKY	-	-	2.9	2.90
rs32239074	1:189860163	MA0046	HNF1A	+	1.7	-	1.70

rs32239074	1:189860163	M00016	E74A	-	3	4.6	1.60
rs32038280	1:189865403	T00368	HNF-1alpha-A	-	-	4.5	4.50
rs32038280	1:189865403	MA0046	HNF1A	-	-	4.1	4.10
rs32038280	1:189865403	M00747	IRF-1	-	3.4	-	3.40
rs32038280	1:189865403	M00790	HNF1	-	2.8	5.6	2.80
rs32038280	1:189865403	M00451	Nkx3-1	+	3.1	5.2	2.10
rs32038280	1:189865403	MA0063	Nkx2-5	+	2.1	-	2.10
rs3667534	1:189866887	M00454	MRF-2	-	3.7	-	3.70
rs3667534	1:189866887	MA0111	Spz1	+	-	1.3	1.30
rs31081923	1:189881827	M00670	NIL	-	-	1	1.00
rs31690423	1:189884459	M00753	RCS1	+	-	3.3	3.30
rs31690423	1:189884459	M00640	HOXA4	-	-	1.3	1.30
rs30473053	1:189885064	T00715	RAP1	-	-	4.2	4.20
rs30473053	1:189885064	T00725	REB1	+	-	3.6	3.60
rs30473053	1:189885064	M00480	LUN-1	+	-	2.5	2.50
rs30473053	1:189885064	MA0028	ELK1	+	-	2	2.00
rs3673367	1:189886643						
rs3683961	1:189903263	M00274	STE11	+	1.9	3.5	1.60
rs3683961	1:189903263	MA0073	RREB1	-	1.2	-	1.20
rs32085863	1:189903441	T02338	Sp3	+	-	3.9	3.90
rs32085863	1:189903441	T01841	NIL	-	1.1	2.6	1.50
rs32085863	1:189903441	T01842	NIL	-	1.1	2.6	1.50
rs2228901	1:189905663	MA0073	RREB1	-	1.9	-	1.90
rs2228901	1:189905663	T00806	TEF-1	+	1.5	-	1.50
rs2228901	1:189905663	MA0020	Dof2	-	1.5	-	1.50
rs2228901	1:189905663	MA0021	Dof3	-	1.5	-	1.50
rs30572892	1:189906487	T03458	Crx	+	5.1	7	1.90
rs30572892	1:189906487	MA0022	dl_1	+	2.9	1.7	1.20
rs31400926	1:189906947	M00697	HBP-1b	+	-	3.5	3.50
rs31400926	1:189906947	T00114	c-Ets-1 54	-	3	-	3.00

rs31400926	1:189906947	T00244	Egr-1	+	4.7	2.3	2.40
rs31400926	1:189906947	T00899	WT1	-	4.5	2.4	2.10
rs31400926	1:189906947	M00706	TFII-I	-	1.3	-	1.30
rs31400926	1:189906947	M00733	SMAD4	-	3.3	2.2	1.10
rs32757999	1:189907183	MA0078	Sox17	-	3.8	-	3.80
rs32757999	1:189907183	M00063	IRF-2	+	-	3.3	3.30
rs32757999	1:189907183	M00729	Cdx-2	-	3.1	-	3.10
rs32757999	1:189907183	M00699	ICSBP	+	3	-	3.00
rs32757999	1:189907183	M00664	STE12	+	2	-	2.00
rs32757999	1:189907183	MA0045	HMG-I/Y	+	-	1.8	1.80
rs32757999	1:189907183	MA0084	SRY	+	1.8	-	1.80
rs30993521	1:190011782	T01422	ste11	-	-	4.4	4.40
rs30993521	1:190011782	M00274	STE11	-	2.6	6.5	3.90
rs3694567	1:190013851	T01973	NIL	+	7	2.1	4.90
rs3694567	1:190013851	M00721	CACCC-binding factor	+	3.4	-	3.40
rs3694567	1:190013851	T01526	Brachyury	-	4.8	2.1	2.70
rs3694567	1:190013851	M00150	Brachyury	-	5	2.4	2.60

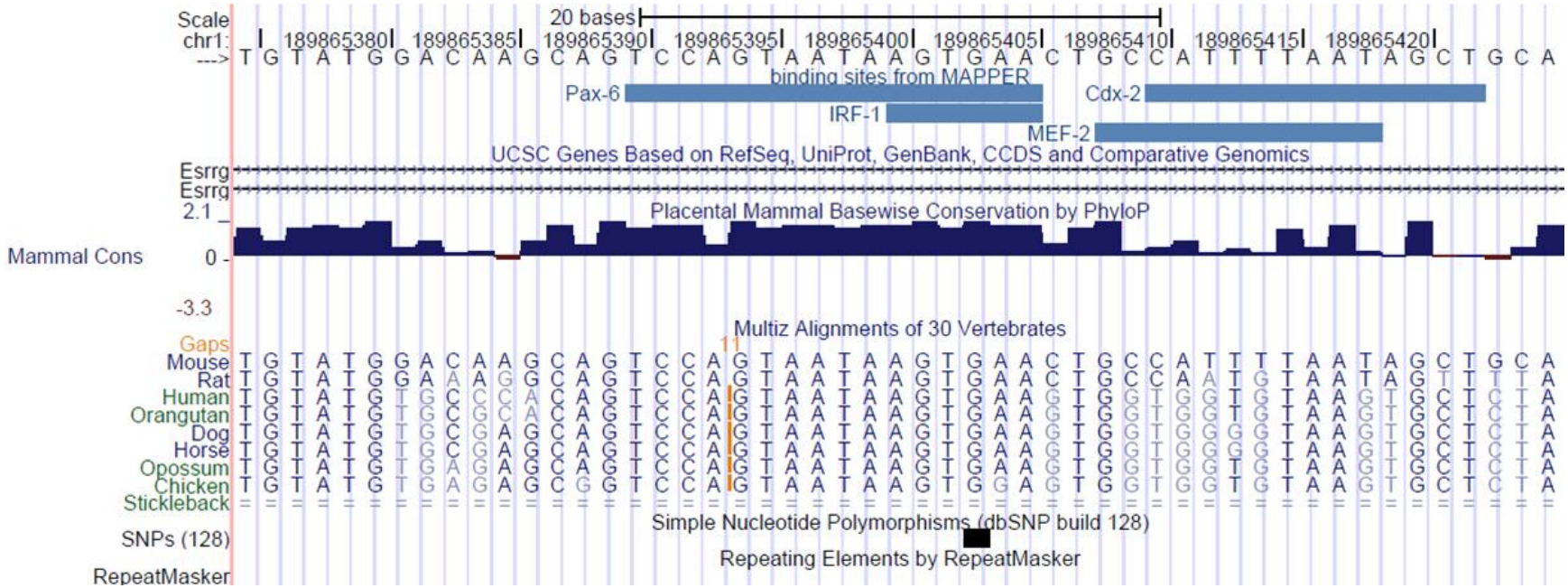

Figure A-2. Alignment of rs32038280 with transcription factor binding sites.

APPENDIX B
GENERATION OF A VECTOR FOR ECTOPIC EXPRESSION OF *ESRRG* IN PRIMARY $CD4^+$ T CELLS

B6 $CD4^+$ T cells were used to clone *Esrrg* without a stop codon in front of a 2A peptide followed by *gfp*. This construct was subcloned into a pCDNA3 mammalian expression vector and tested in 293 cells along with si*Esrrg* (ABI). RT-PCR and qPCR (Figure B-1) showed high levels of *Esrrg* expression that was specifically knocked down by si*Esrrg*. Protein expression and knock-down were also detected by microscopy, western blot, and FACS (Figure B-2)

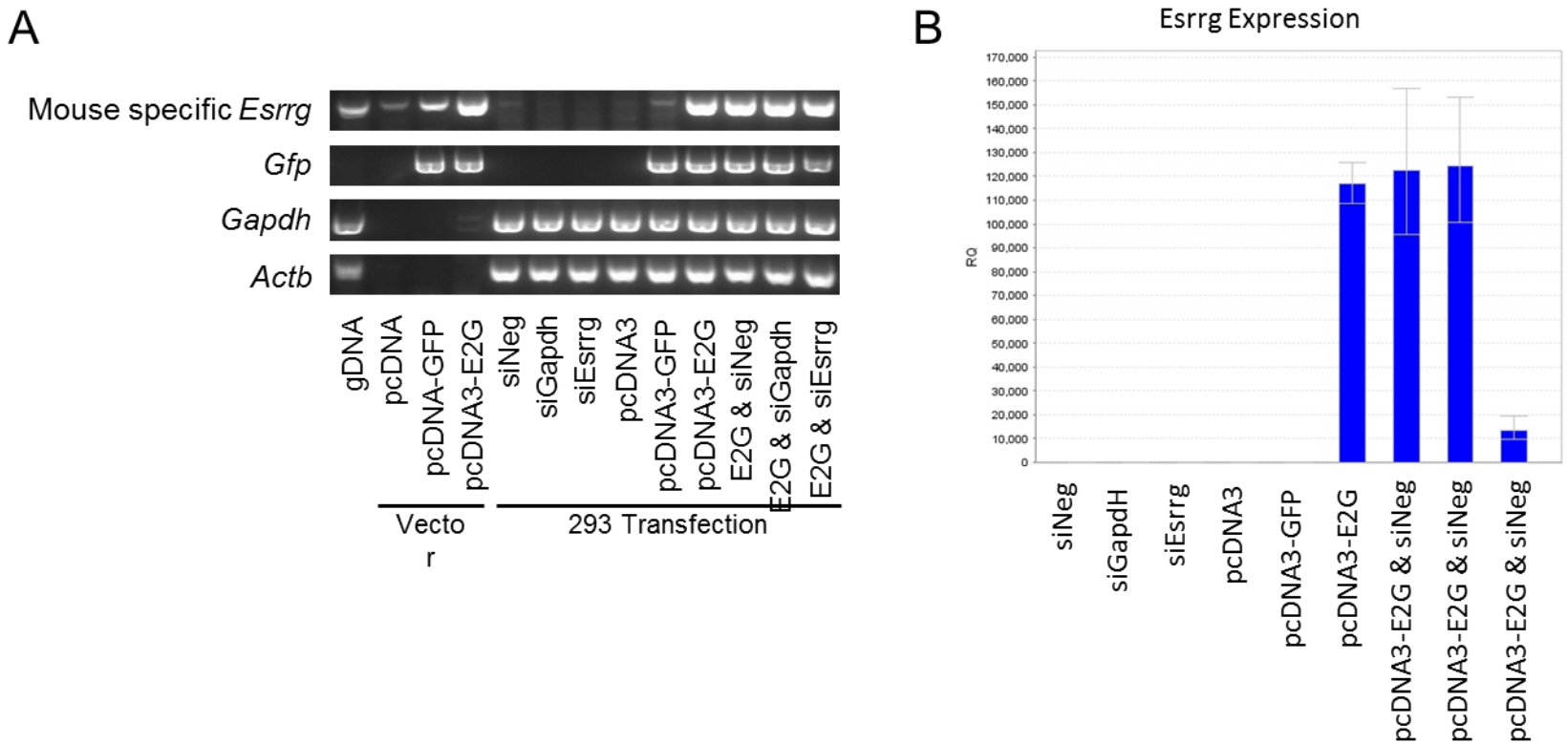

Figure B-1. Gene expression in 293 cells transfected with *Esrrg*. E2G = *Esrrg-2A-gfp*. (A) RT-PCR, (B) qPCR.

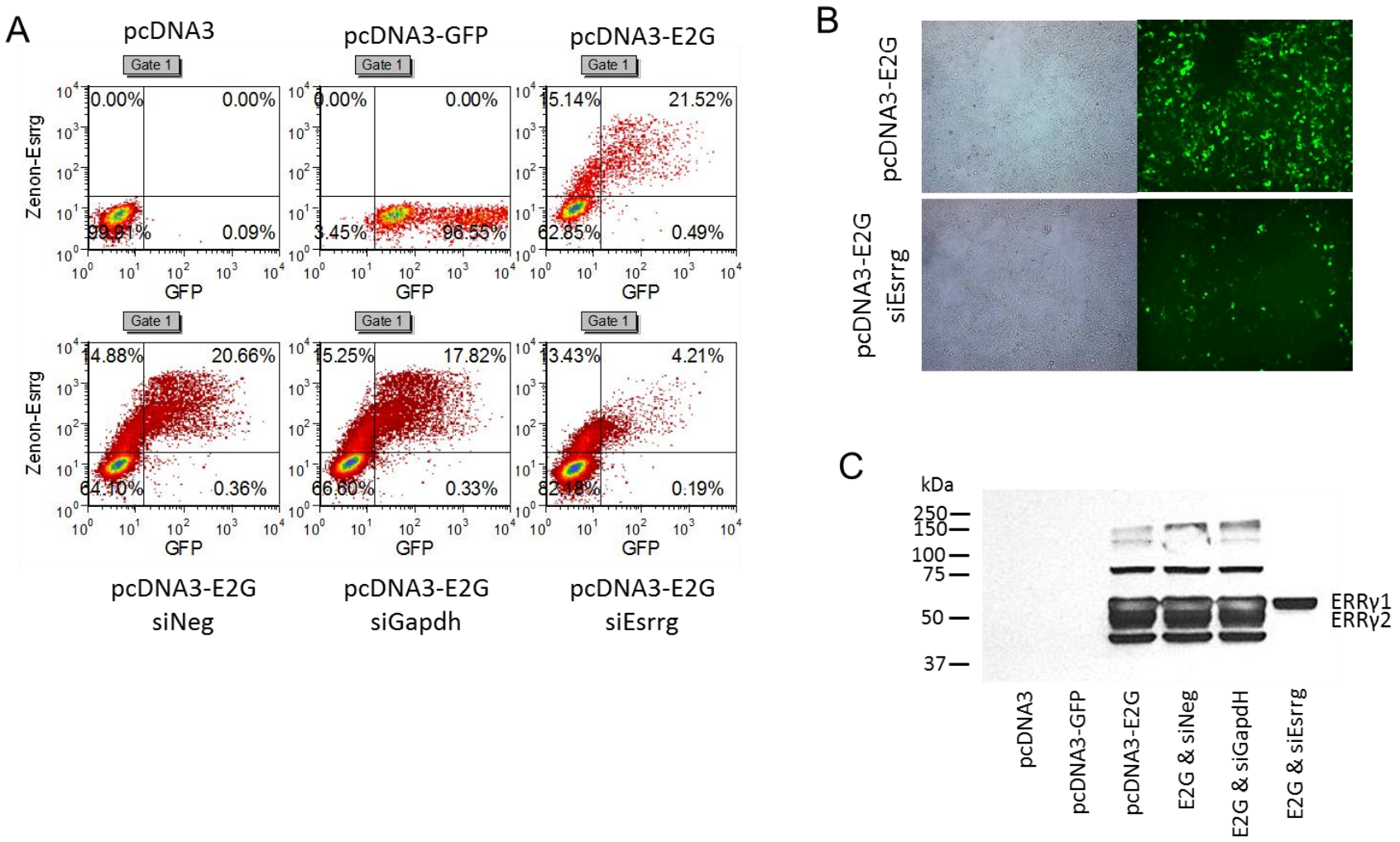

Figure B-2. Protein expression in 293 cells transfected with *Esrrg*. E2G = *Esrrg-2A-gfp.* (A) FACS, (B) Microscopy, (C) Western blot

LIST OF REFERENCES

1. Barrat, F., T. Meeker, J. Gregorio, J. Chan, S. Uematsu, S. Akira, B. Chang, O. Duramad, and R. Coffman. 2005. Nucleic acids of mammalian origin can act as endogenous ligands for Toll-like receptors and may promote systemic lupus erythematosus. *J Exp Med* 202: 1131-1139.

2. Lam, G. K., and M. Petri. 2005. Assessment of systemic lupus erythematosus. *Clin Exp Rheumatol* 23: S120-132.

3. Hochberg, M. C. 1997. Updating the American College of Rheumatology revised criteria for the classification of systemic lupus erythematosus. *Arthritis Rheum* 40: 1725.

4. Tan, E. M., A. S. Cohen, J. F. Fries, A. T. Masi, D. J. McShane, N. F. Rothfield, J. G. Schaller, N. Talal, and R. J. Winchester. 1982. The 1982 revised criteria for the classification of systemic lupus erythematosus. *Arthritis Rheum* 25: 1271-1277.

5. Petri, M., and L. Magder. 2004. Classification criteria for systemic lupus erythematosus: a review. *Lupus* 13: 829-837.

6. Yildirim-Toruner, C., and B. Diamond. 2011. Current and novel therapeutics in the treatment of systemic lupus erythematosus. *J Allergy Clin Immunol* 127: 303-312; quiz 313-304.

7. Pascual, V., L. Farkas, and J. Banchereau. 2006. Systemic lupus erythematosus: all roads lead to type I interferons. *Curr Opin Immunol* 18: 676-682.

8. Jacobi, A. M., W. Huang, T. Wang, W. Freimuth, I. Sanz, R. Furie, M. Mackay, C. Aranow, B. Diamond, and A. Davidson. 2010. Effect of long-term belimumab treatment on B cells in systemic lupus erythematosus: extension of a phase II, double-blind, placebo-controlled, dose-ranging study. *Arthritis Rheum* 62: 201-210.

9. Wallace, D. J., W. Stohl, R. A. Furie, J. R. Lisse, J. D. McKay, J. T. Merrill, M. A. Petri, E. M. Ginzler, W. W. Chatham, W. J. McCune, V. Fernandez, M. R. Chevrier, Z. J. Zhong, and W. W. Freimuth. 2009. A phase II, randomized, double-blind, placebo-controlled, dose-ranging study of belimumab in patients with active systemic lupus erythematosus. *Arthritis Rheum* 61: 1168-1178.

10. Kelly, J. A., K. L. Moser, and J. B. Harley. 2002. The genetics of systemic lupus erythematosus: putting the pieces together. *Genes Immun* 3 Suppl 1: S71-85.

11. Deapen, D., A. Escalante, L. Weinrib, D. Horwitz, B. Bachman, P. Roy-Burman, A. Walker, and T. M. Mack. 1992. A revised estimate of twin concordance in systemic lupus erythematosus. *Arthritis Rheum* 35: 311-318.

12. Sestak, A. L., T. S. Shaver, K. L. Moser, B. R. Neas, and J. B. Harley. 1999. Familial aggregation of lupus and autoimmunity in an unusual multiplex pedigree. *J Rheumatol* 26: 1495-1499.

13. Fessel, W. J. 1974. Systemic lupus erythematosus in the community. Incidence, prevalence, outcome, and first symptoms; the high prevalence in black women. *Arch Intern Med* 134: 1027-1035.

14. Kaslow, R. A., and A. T. Masi. 1978. Age, sex, and race effects on mortality from systemic lupus erythematosus in the United States. *Arthritis Rheum* 21: 473-479.

15. Walker, S. E. 2011. Estrogen and autoimmune disease. *Clin Rev Allergy Immunol* 40: 60-65.

16. Petri, M. 2008. Sex hormones and systemic lupus erythematosus. *Lupus* 17: 412-415.

17. Roubinian, J., N. Talal, J. Greenspan, J. Goodman, and P. Siiteri. 1978. Effect of castration and sex hormone treatment on survival, anti-nucleic acid antibodies, and glomerulonephritis in NZB/NZW F1 mice. *J Exp Med* 147: 1568-1583.

18. Bynoté, K. K., J. M. Hackenberg, K. S. Korach, D. B. Lubahn, P. H. Lane, and K. A. Gould. 2008. Estrogen receptor-alpha deficiency attenuates autoimmune disease in (NZB x NZW)F1 mice. *Genes Immun* 9: 137-152.

19. Scofield, R. H., G. R. Bruner, B. Namjou, R. P. Kimberly, R. Ramsey-Goldman, M. Petri, J. D. Reveille, G. S. Alarcón, L. M. Vilá, J. Reid, B. Harris, S. Li, J. A. Kelly, and J. B. Harley. 2008. Klinefelter's syndrome (47,XXY) in male systemic lupus erythematosus patients: support for the notion of a gene-dose effect from the X chromosome. *Arthritis Rheum* 58: 2511-2517.

20. Pisitkun, P., J. A. Deane, M. J. Difilippantonio, T. Tarasenko, A. B. Satterthwaite, and S. Bolland. 2006. Autoreactive B Cell Responses to RNA-Related Antigens Due to TLR7 Gene Duplication. *Science* 312: 1669-1672.

21. Subramanian, S., K. Tus, Q.-Z. Li, A. Wang, X.-H. Tian, J. Zhou, C. Liang, G. Bartov, L. D. McDaniel, X. J. Zhou, R. A. Schultz, and E. K. Wakeland. 2006. A Tlr7 translocation accelerates systemic autoimmunity in murine lupus. *Proc Natl Acad Sci U S A* 103: 9970-9975.

22. Deane, J. A., P. Pisitkun, R. S. Barrett, L. Feigenbaum, T. Town, Jerrold M. Ward, R. A. Flavell, and S. Bolland. 2007. Control of Toll-like Receptor 7 Expression Is Essential to Restrict Autoimmunity and Dendritic Cell Proliferation. *Immunity* 27: 801-810.

23. Fairhurst, A. M., S. h. Hwang, A. Wang, X. H. Tian, C. Boudreaux, X. Zhou, J. Casco, Q. Z. Li, J. Connolly, and E. Wakeland. 2008. Yaa autoimmune

phenotypes are conferred by overexpression of TLR7. *Eur J Immunol* 38: 1971-1978.

24. Santiago-Raber, M.-L., S. Kikuchi, P. Borel, S. Uematsu, S. Akira, B. L. Kotzin, and S. Izui. 2008. Evidence for Genes in Addition to Tlr7 in the Yaa Translocation Linked with Acceleration of Systemic Lupus Erythematosus. *J Immunol* 181: 1556-1562.

25. Moser, K., J. Kelly, C. Lessard, and J. Harley. 2009. Recent insights into the genetic basis of systemic lupus erythematosus. *Genes Immun* 10: 373-379.

26. Sestak, A. L., B. G. Fürnrohr, J. B. Harley, J. T. Merrill, and B. Namjou. 2011. The genetics of systemic lupus erythematosus and implications for targeted therapy. *Ann Rheum Dis* 70 Suppl 1: i37-43.

27. Flint, J., W. Valdar, S. Shifman, and R. Mott. 2005. Strategies for mapping and cloning quantitative trait genes in rodents. *Nat Rev Genet* 6: 271-286.

28. Wakeland, E., L. Morel, K. Achey, M. Yui, and J. Longmate. 1997. Speed congenics: a classic technique in the fast lane (relatively speaking). *Immunol Today* 18: 472-477.

29. Wandstrat, A. E., C. Nguyen, N. Limaye, A. Y. Chan, S. Subramanian, X. H. Tian, Y. S. Yim, A. Pertsemlidis, H. R. Garner, L. Morel, and E. K. Wakeland. 2004. Association of Extensive Polymorphisms in the SLAM/CD2 Gene Cluster with Murine Lupus. *Immunity* 21: 769-780.

30. Kumar, K. R., L. Li, M. Yan, M. Bhaskarabhatla, A. B. Mobley, C. Nguyen, J. M. Mooney, J. D. Schatzle, E. K. Wakeland, and C. Mohan. 2006. Regulation of B Cell Tolerance by the Lupus Susceptibility Gene Ly108. *Science* 312: 1665-1669.

31. Min-Oo, G., A. Fortin, G. Pitari, M. Tam, M. M. Stevenson, and P. Gros. 2007. Complex genetic control of susceptibility to malaria: positional cloning of the Char9 locus. *J Exp Med* 204: 511-524.

32. Kissler, S., P. Stern, K. Takahashi, K. Hunter, L. B. Peterson, and L. S. Wicker. 2006. In vivo RNA interference demonstrates a role for Nramp1 in modifying susceptibility to type 1 diabetes. *Nat Genet* 38: 479-483.

33. Rudofsky, U. H., B. D. Evans, S. L. Balaban, V. D. Mottironi, and A. E. Gabrielsen. 1993. Differences in expression of lupus nephritis in New Zealand mixed H-2z homozygous inbred strains of mice derived from New Zealand black and New Zealand white mice. Origins and initial characterization. *Lab Invest* 68: 419-426.

34. Morel, L., U. H. Rudofsky, J. A. Longmate, J. Schiffenbauer, and E. K. Wakeland. 1994. Polygenic control of susceptibility to murine systemic lupus erythematosus. *Immunity* 1: 219-229.

35. Morel, L., C. Mohan, Y. Yu, B. P. Croker, N. Tian, A. Deng, and E. K. Wakeland. 1997. Functional dissection of systemic lupus erythematosus using congenic mouse strains. *J Immunol* 158: 6019-6028.

36. Morel, L., B. P. Croker, K. R. Blenman, C. Mohan, G. Huang, G. Gilkeson, and E. K. Wakeland. 2000. Genetic reconstitution of systemic lupus erythematosus immunopathology with polycongenic murine strains. *Proc Natl Acad Sci U S A* 97: 6670-6675.

37. Mohan, C., L. Morel, P. Yang, and E. Wakeland. 1997. Genetic dissection of systemic lupus erythematosus pathogenesis: Sle2 on murine chromosome 4 leads to B cell hyperactivity. *J Immunol* 159: 454-465.

38. Xu, Z., H. H. Potula, A. Vallurupalli, D. Perry, H. Baker, B. P. Croker, I. Dozmorov, and L. Morel. 2011. Cyclin-Dependent Kinase Inhibitor Cdkn2c Regulates B Cell Homeostasis and Function in the NZM2410-Derived Murine Lupus Susceptibility Locus Sle2c1. *J Immunol* 186: 6673-6682.

39. Sobel, E., L. Morel, R. Baert, C. Mohan, J. Schiffenbauer, and E. Wakeland. 2002. Genetic dissection of systemic lupus erythematosus pathogenesis: evidence for functional expression of Sle3/5 by non-T cells. *J Immunol* 169: 4025-4032.

40. Liu, K., Q. Z. Li, Y. Yu, C. Liang, S. Subramanian, Z. Zeng, H. W. Wang, C. Xie, X. J. Zhou, C. Mohan, and E. K. Wakeland. 2007. Sle3 and Sle5 can independently couple with Sle1 to mediate severe lupus nephritis. *Genes Immun* 8: 634-645.

41. Li, Q. Z., J. Zhou, R. Yang, M. Yan, Q. Ye, K. Liu, S. Liu, X. Shao, L. Li, X. J. Zhou, E. K. Wakeland, and C. Mohan. 2009. The lupus-susceptibility gene kallikrein downmodulates antibody-mediated glomerulonephritis. *Genes Immun* 10: 503-508.

42. Liu, K., Q. Li, A. Delgado-Vega, A. Abelson, E. Sánchez, J. Kelly, L. Li, Y. Liu, J. Zhou, M. Yan, Q. Ye, S. Liu, C. Xie, X. Zhou, S. Chung, B. Pons-Estel, T. Witte, E. de Ramón, S. Bae, N. Barizzone, G. Sebastiani, J. Merrill, P. Gregersen, G. Gilkeson, R. Kimberly, T. Vyse, I. Kim, S. D'Alfonso, J. Martin, J. Harley, L. Criswell, E. Wakeland, M. Alarcón-Riquelme, C. Mohan, P. S. Group, I. C. Group, G. C. Group, S. C. Group, A. C. Group, and S. Consortium. 2009. Kallikrein genes are associated with lupus and glomerular basement membrane-specific antibody-induced nephritis in mice and humans. *J Clin Invest* 119: 911-923.

43. Mohan, C., E. Alas, L. Morel, P. Yang, and E. K. Wakeland. 1998. Genetic Dissection of SLE Pathogenesis . Sle1 on Murine Chromosome 1 Leads to a Selective Loss of Tolerance to H2A/H2B/DNA Subnucleosomes. *J Clin Invest* 101: 1362-1372.

44. Wakeland, E. K., K. Liu, R. R. Graham, and T. W. Behrens. 2001. Delineating the Genetic Basis of Systemic Lupus Erythematosus. *Immunity* 15: 397-408.

45. Wakeland, E. K., A. E. Wandstrat, K. Liu, and L. Morel. 1999. Genetic dissection of systemic lupus erythematosus. *Curr Opin Immunol* 11: 701-707.

46. Hogarth, M. B., J. H. Slingsby, P. J. Allen, E. M. Thompson, P. Chandler, K. A. Davies, E. Simpson, B. J. Morley, and M. J. Walport. 1998. Multiple Lupus Susceptibility Loci Map to Chromosome 1 in BXSB Mice. *J Immunol* 161: 2753-2761.

47. Perry, D., A. Sang, Y. Yin, Y. Y. Zheng, and L. Morel. 2011. Murine models of systemic lupus erythematosus. *J Biomed Biotechnol* 2011: 271694.

48. Waters, S. T., S. M. Fu, F. Gaskin, U. S. Deshmukh, S. S. Sung, C. C. Kannapell, K. S. K. Tung, S. B. McEwen, and M. McDuffie. 2001. NZM2328: A New Mouse Model of Systemic Lupus Erythematosus with Unique Genetic Susceptibility Loci. *Clinical Immunol* 100: 372-383.

49. Vyse, T. J., S. J. Rozzo, C. G. Drake, S. Izui, and B. L. Kotzin. 1997. Control of multiple autoantibodies linked with a lupus nephritis susceptibility locus in New Zealand black mice. *J Immunol* 158: 5566-5574.

50. Morel, L., K. R. Blenman, B. P. Croker, and E. K. Wakeland. 2001. The major murine systemic lupus erythematosus susceptibility locus, Sle1, is a cluster of functionally related genes. *Proc Natl Acad Sci U S A* 98: 1787-1792.

51. Giles, B. M., S. N. Tchepeleva, J. J. Kachinski, K. Ruff, B. P. Croker, L. Morel, and S. A. Boackle. 2007. Augmentation of NZB Autoimmune Phenotypes by the Sle1c Murine Lupus Susceptibility Interval. *J Immunol* 178: 4667-4675.

52. Chen, Y., D. Perry, S. A. Boackle, E. S. Sobel, H. Molina, B. P. Croker, and L. Morel. 2005. Several Genes Contribute to the Production of Autoreactive B and T Cells in the Murine Lupus Susceptibility Locus Sle1c. *J Immunol* 175: 1080-1089.

53. Boackle, S. A., V. M. Holers, X. J. Chen, G. Szakonyi, D. R. Karp, E. K. Wakeland, and L. Morel. 2001. Cr2, a candidate gene in the murine Sle1c lupus susceptibility locus, encodes a dysfunctional protein. *Immunity* 15: 775-785.

54. Tchepeleva, S. N., J. M. Thurman, K. Ruff, S. J. Perkins, L. Morel, and S. A. Boackle. 2010. An allelic variant of Crry in the murine Sle1c lupus susceptibility interval is not impaired in its ability to regulate complement activation. *J Immunol* 185: 2331-2339.

55. Sestak, A., S. Nath, A. Sawalha, and J. Harley. 2007. Current status of lupus genetics. *Arthritis Res Ther* 9: 210.

56. Mosmann, T. R., H. Cherwinski, M. W. Bond, M. A. Giedlin, and R. L. Coffman. 1986. Two types of murine helper T cell clone. I. Definition according to profiles of lymphokine activities and secreted proteins. *J Immunol* 136: 2348-2357.

57. Zhu, J., H. Yamane, and W. E. Paul. 2010. Differentiation of effector CD4 T cell populations (*). *Annu Rev Immunol* 28: 445-489.

58. Theofilopoulos, A. N., S. Koundouris, D. H. Kono, and B. R. Lawson. 2001. The role of IFN-gamma in systemic lupus erythematosus: a challenge to the Th1/Th2 paradigm in autoimmunity. *Arthritis Res* 3: 136-141.

59. Curotto de Lafaille, M. A., and J. J. Lafaille. 2009. Natural and adaptive foxp3+ regulatory T cells: more of the same or a division of labor? *Immunity* 30: 626-635.

60. Belkaid, Y., and W. Chen. 2010. Regulatory ripples. *Nat Immunol* 11: 1077-1078.

61. Roncarolo, M. G., S. Gregori, M. Battaglia, R. Bacchetta, K. Fleischhauer, and M. K. Levings. 2006. Interleukin-10-secreting type 1 regulatory T cells in rodents and humans. *Immunol Rev* 212: 28-50.

62. Collison, L. W., V. Chaturvedi, A. L. Henderson, P. R. Giacomin, C. Guy, J. Bankoti, D. Finkelstein, K. Forbes, C. J. Workman, S. A. Brown, J. E. Rehg, M. L. Jones, H. T. Ni, D. Artis, M. J. Turk, and D. A. Vignali. 2010. IL-35-mediated induction of a potent regulatory T cell population. *Nat Immunol* 11: 1093-1101.

63. Cua, D., J. Sherlock, Y. Chen, C. Murphy, B. Joyce, B. Seymour, L. Lucian, W. To, S. Kwan, T. Churakova, S. Zurawski, M. Wiekowski, S. Lira, D. Gorman, R. Kastelein, and J. Sedgwick. 2003. Interleukin-23 rather than interleukin-12 is the critical cytokine for autoimmune inflammation of the brain. *Nature* 421: 744-748.

64. Perry, D., A. Peck, W. Carcamo, L. Morel, and C. Nguyen. 2011. The Current Concept of TH17 Cells and Their Expanding Role in Systemic Lupus Erythematosus. *Arthritis* 2011: 10.

65. Dardalhon, V., A. Awasthi, H. Kwon, G. Galileos, W. Gao, R. A. Sobel, M. Mitsdoerffer, T. B. Strom, W. Elyaman, I. C. Ho, S. Khoury, M. Oukka, and V. K. Kuchroo. 2008. IL-4 inhibits TGF-beta-induced Foxp3+ T cells and, together with TGF-beta, generates IL-9+ IL-10+ Foxp3(-) effector T cells. *Nat Immunol* 9: 1347-1355.

66. Veldhoen, M., C. Uyttenhove, J. van Snick, H. Helmby, A. Westendorf, J. Buer, B. Martin, C. Wilhelm, and B. Stockinger. 2008. Transforming growth factor-beta 'reprograms' the differentiation of T helper 2 cells and promotes an interleukin 9-producing subset. *Nat Immunol* 9: 1341-1346.

67. Duhen, T., R. Geiger, D. Jarrossay, A. Lanzavecchia, and F. Sallusto. 2009. Production of interleukin 22 but not interleukin 17 by a subset of human skin-homing memory T cells. *Nat Immunol* 10: 857-863.

68. Trifari, S., C. D. Kaplan, E. H. Tran, N. K. Crellin, and H. Spits. 2009. Identification of a human helper T cell population that has abundant production of interleukin 22 and is distinct from T(H)-17, T(H)1 and T(H)2 cells. *Nat Immunol* 10: 864-871.

69. Crotty, S. 2011. Follicular helper CD4 T cells (TFH). *Annu Rev Immunol* 29: 621-663.

70. Hooks, J. J., H. M. Moutsopoulos, S. A. Geis, N. I. Stahl, J. L. Decker, and A. L. Notkins. 1979. Immune interferon in the circulation of patients with autoimmune disease. *N Engl J Med* 301: 5-8.

71. Tucci, M., L. Lombardi, H. B. Richards, F. Dammacco, and F. Silvestris. 2008. Overexpression of interleukin-12 and T helper 1 predominance in lupus nephritis. *Clin Exp Immunol* 154: 247-254.

72. Calvani, N., H. B. Richards, M. Tucci, G. Pannarale, and F. Silvestris. 2004. Up-regulation of IL-18 and predominance of a Th1 immune response is a hallmark of lupus nephritis. *Clin Exp Immunol* 138: 171-178.

73. Tokano, Y., S. Morimoto, H. Kaneko, H. Amano, K. Nozawa, Y. Takasaki, and H. Hashimoto. 1999. Levels of IL-12 in the sera of patients with systemic lupus erythematosus (SLE)--relation to Th1- and Th2-derived cytokines. *Clin Exp Immunol* 116: 169-173.

74. Enghard, P., D. Langnickel, and G. Riemekasten. 2006. T cell cytokine imbalance towards production of IFN-gamma and IL-10 in NZB/W F1 lupus-prone mice is associated with autoantibody levels and nephritis. *Scand J Rheumatol* 35: 209-216.

75. Haas, C., B. Ryffel, and M. Le Hir. 1998. IFN-gamma receptor deletion prevents autoantibody production and glomerulonephritis in lupus-prone (NZB x NZW)F1 mice. *J Immunol* 160: 3713-3718.

76. Takahashi, S., L. Fossati, M. Iwamoto, R. Merino, R. Motta, T. Kobayakawa, and S. Izui. 1996. Imbalance towards Th1 predominance is associated with acceleration of lupus-like autoimmune syndrome in MRL mice. *J Clin Invest* 97: 1597-1604.

77. Richards, H. B., M. Satoh, J. C. Jennette, B. P. Croker, H. Yoshida, and W. H. Reeves. 2001. Interferon-gamma is required for lupus nephritis in mice treated with the hydrocarbon oil pristane. *Kidney Int* 60: 2173-2180.

78. Baudino, L., S. Azeredo da Silveira, M. Nakata, and S. Izui. 2006. Molecular and cellular basis for pathogenicity of autoantibodies: lessons from murine monoclonal autoantibodies. *Springer Semin Immunopathol* 28: 175-184.

79. Korn, T., E. Bettelli, M. Oukka, and V. Kuchroo. 2009. IL-17 and Th17 Cells. *Annu Rev Immunol* 27: 485-517.

80. Murphy, C. A., C. L. Langrish, Y. Chen, W. Blumenschein, T. McClanahan, R. A. Kastelein, J. D. Sedgwick, and D. J. Cua. 2003. Divergent pro- and antiinflammatory roles for IL-23 and IL-12 in joint autoimmune inflammation. *J Exp Med* 198: 1951-1957.

81. Morse, H. C., T. M. Chused, J. W. Hartley, B. J. Mathieson, S. O. Sharrow, and B. A. Taylor. 1979. Expression of xenotropic murine leukemia viruses as cell-surface gp70 in genetic crosses between strains DBA/2 and C57BL/6. *J Exp Med* 149: 1183-1196.

82. Taylor, B. A., C. Wnek, B. S. Kotlus, N. Roemer, T. MacTaggart, and S. J. Phillips. 1999. Genotyping new BXD recombinant inbred mouse strains and comparison of BXD and consensus maps. *Mamm Genome* 10: 335-348.

83. Mountz, J. D., P. Yang, Q. Wu, J. Zhou, A. Tousson, A. Fitzgerald, J. Allen, X. Wang, S. Cartner, W. E. Grizzle, N. Yi, L. Lu, R. W. Williams, and H. C. Hsu. 2005. Genetic Segregation of Spontaneous Erosive Arthritis and Generalized Autoimmune Disease in the BXD2 Recombinant Inbred Strain of Mice. *Scand J Immunol* 61: 128-138.

84. Hsu, H. C., T. Zhou, H. Kim, S. Barnes, P. Yang, Q. Wu, J. Zhou, B. A. Freeman, M. Luo, and J. D. Mountz. 2006. Production of a novel class of polyreactive pathogenic autoantibodies in BXD2 mice causes glomerulonephritis and arthritis. *Arthritis Rheum* 54: 343-355.

85. Hsu, H.-C., P. Yang, J. Wang, Q. Wu, R. Myers, J. Chen, J. Yi, T. Guentert, A. Tousson, A. L. Stanus, T.-v. L. Le, R. G. Lorenz, H. Xu, J. K. Kolls, R. H. Carter, D. D. Chaplin, R. W. Williams, and J. D. Mountz. 2008. Interleukin 17-producing T helper cells and interleukin 17 orchestrate autoreactive germinal center development in autoimmune BXD2 mice. *Nat Immunol* 9: 166-175.

86. Xie, S., J. Li, J. Wang, Q. Wu, P. Yang, H. Hsu, L. Smythies, and J. Mountz. 2010. IL-17 activates the canonical NF-kappaB signaling pathway in autoimmune B cells of BXD2 mice to upregulate the expression of regulators of G-protein signaling 16. *J Immunol* 184: 2289-2296.

87. Koelle, M. 1997. A new family of G-protein regulators - the RGS proteins. *Curr Opin Cell Biol* 9: 143-147.

88. Shi, G., K. Harrison, G. Wilson, C. Moratz, and J. Kehrl. 2002. RGS13 regulates germinal center B lymphocytes responsiveness to CXC chemokine ligand (CXCL)12 and CXCL13. *J Immunol* 169: 2507-2515.

89. Allen, C., K. Ansel, C. Low, R. Lesley, H. Tamamura, N. Fujii, and J. Cyster. 2004. Germinal center dark and light zone organization is mediated by CXCR4 and CXCR5. *Nat Immunol* 5: 943-952.

90. Allen, C., T. Okada, and J. Cyster. 2007. Germinal-center organization and cellular dynamics. *Immunity* 27: 190-202.

91. Cohen, P., and R. Eisenberg. 1991. Lpr and gld: single gene models of systemic autoimmunity and lymphoproliferative disease. *Annu Rev Immunol* 9: 243-269.

92. Adachi, M., R. Watanabe-Fukunaga, and S. Nagata. 1993. Aberrant transcription caused by the insertion of an early transposable element in an intron of the Fas antigen gene of lpr mice. *Proc Natl Acad Sci U S A* 90: 1756-1760.

93. Kono, D., and A. Theofilopoulos. 2006. Genetics of SLE in mice. *Springer Semin Immunopathol* 28: 83-96.

94. Zhang, Z., V. Kyttaris, and G. Tsokos. 2009. The role of IL-23/IL-17 axis in lupus nephritis. *J Immunol* 183: 3160-3169.

95. Kyttaris, V., Z. Zhang, V. Kuchroo, M. Oukka, and G. Tsokos. 2010. Cutting edge: IL-23 receptor deficiency prevents the development of lupus nephritis in C57BL/6-lpr/lpr mice. *J Immunol* 184: 4605-4609.

96. Kaliyaperumal, A., C. Mohan, W. Wu, and S. Datta. 1996. Nucleosomal peptide epitopes for nephritis-inducing T helper cells of murine lupus. *J Exp Med* 183: 2459-2469.

97. Kang, H., M. Liu, and S. Datta. 2007. Low-dose peptide tolerance therapy of lupus generates plasmacytoid dendritic cells that cause expansion of autoantigen-specific regulatory T cells and contraction of inflammatory Th17 cells. *J Immunol* 178: 7849-7858.

98. Wu, H., F. Quintana, and H. Weiner. 2008. Nasal anti-CD3 antibody ameliorates lupus by inducing an IL-10-secreting CD4+ CD25- LAP+ regulatory T cell and is associated with down-regulation of IL-17+ CD4+ ICOS+ CXCR5+ follicular helper T cells. *J Immunol* 181: 6038-6050.

99. Wu, H., E. Center, G. Tsokos, and H. Weiner. 2009. Suppression of murine SLE by oral anti-CD3: inducible CD4+CD25-LAP+ regulatory T cells control the expansion of IL-17+ follicular helper T cells. *Lupus* 18: 586-596.

100. Jacob, N., H. Yang, L. Pricop, Y. Liu, X. Gao, S. Zheng, J. Wang, H. Gao, C. Putterman, M. Koss, W. Stohl, and C. Jacob. 2009. Accelerated pathological and clinical nephritis in systemic lupus erythematosus-prone New Zealand Mixed 2328 mice doubly deficient in TNF receptor 1 and TNF receptor 2 via a Th17-associated pathway. *J Immunol* 182: 2532-2541.

101. Wong, C., L. Lit, L. Tam, E. Li, P. Wong, and C. Lam. 2008. Hyperproduction of IL-23 and IL-17 in patients with systemic lupus erythematosus: implications for Th17-mediated inflammation in auto-immunity. *Clin Immunol* 127: 385-393.

102. Chen, X., Y. Yu, H. Deng, J. Sun, Z. Dai, Y. Wu, and M. Yang. 2010. Plasma IL-17A is increased in new-onset SLE patients and associated with disease activity. *J Clin Immunol* 30: 221-225.

103. Shah, K., W. Lee, S. Lee, S. Kim, S. Kang, J. Craft, and I. Kang. 2010. Dysregulated balance of Th17 and Th1 cells in systemic lupus erythematosus. *Arthritis Res Ther* 12: R53.

104. Doreau, A., A. Belot, J. Bastid, B. Riche, M. Trescol-Biemont, B. Ranchin, N. Fabien, P. Cochat, C. Pouteil-Noble, P. Trolliet, I. Durieu, J. Tebib, B. Kassai, S. Ansieau, A. Puisieux, J. Eliaou, and N. Bonnefoy-Bérard. 2009. Interleukin 17 acts in synergy with B cell-activating factor to influence B cell biology and the pathophysiology of systemic lupus erythematosus. *Nat Immunol* 10: 778-785.

105. Crispín, J., M. Oukka, G. Bayliss, R. Cohen, C. Van Beek, I. Stillman, V. Kyttaris, Y. Juang, and G. Tsokos. 2008. Expanded double negative T cells in patients with systemic lupus erythematosus produce IL-17 and infiltrate the kidneys. *J Immunol* 181: 8761-8766.

106. Mok, M., H. Wu, Y. Lo, and C. Lau. 2010. The Relation of Interleukin 17 (IL-17) and IL-23 to Th1/Th2 Cytokines and Disease Activity in Systemic Lupus Erythematosus. *J Rheumatol*.

107. Harada, T., V. Kyttaris, Y. Li, Y. Juang, Y. Wang, and G. Tsokos. 2007. Increased expression of STAT3 in SLE T cells contributes to enhanced chemokine-mediated cell migration. *Autoimmunity* 40: 1-8.

108. Ma, C., G. Chew, N. Simpson, A. Priyadarshi, M. Wong, B. Grimbacher, D. Fulcher, S. Tangye, and M. Cook. 2008. Deficiency of Th17 cells in hyper IgE syndrome due to mutations in STAT3. *J Exp Med* 205: 1551-1557.

109. de Beaucoudrey, L., A. Puel, O. Filipe-Santos, A. Cobat, P. Ghandil, M. Chrabieh, J. Feinberg, H. von Bernuth, A. Samarina, L. Jannière, C. Fieschi, J. Stéphan, C. Boileau, S. Lyonnet, G. Jondeau, V. Cormier-Daire, M. Le Merrer, C. Hoarau, Y. Lebranchu, O. Lortholary, M. Chandesris, F. Tron, E. Gambineri, L. Bianchi, C. Rodriguez-Gallego, S. Zitnik, J. Vasconcelos, M. Guedes, A. Vitor, L. Marodi, H. Chapel, B. Reid, C. Roifman, D. Nadal, J. Reichenbach, I. Caragol, B. Garty, F. Dogu, Y. Camcioglu, S. Gülle, O. Sanal, A. Fischer, L. Abel, B. Stockinger, C. Picard, and J. Casanova. 2008. Mutations in STAT3 and IL12RB1 impair the development of human IL-17-producing T cells. *J Exp Med* 205: 1543-1550.

110. Chen, Z., A. Laurence, and J. O'Shea. 2007. Signal transduction pathways and transcriptional regulation in the control of Th17 differentiation. *Semin Immunol* 19: 400-408.

111. Chun, H., J. Chung, H. Kim, J. Yun, J. Jeon, Y. Ye, S. Kim, H. Park, and C. Suh. 2007. Cytokine IL-6 and IL-10 as biomarkers in systemic lupus erythematosus. *J Clin Immunol* 27: 461-466.

112. Goetzl, E. J., M. C. Huang, J. Kon, K. Patel, J. B. Schwartz, K. Fast, L. Ferrucci, K. Madara, D. D. Taub, and D. L. Longo. 2010. Gender specificity of altered human immune cytokine profiles in aging. *FASEB J* 24: 3580-3589.

113. Khan, D., R. Dai, E. Karpuzoglu, and S. A. Ahmed. 2010. Estrogen increases, whereas IL-27 and IFN-gamma decrease, splenocyte IL-17 production in WT mice. *Eur J Immunol* 40: 2549-2556.

114. Crispín, J., and G. Tsokos. 2009. Human TCR-alpha beta+ CD4- CD8- T cells can derive from CD8+ T cells and display an inflammatory effector phenotype. *J Immunol* 183: 4675-4681.

115. Espinosa, A., V. Dardalhon, S. Brauner, A. Ambrosi, R. Higgs, F. Quintana, M. Sjöstrand, M. Eloranta, J. Ní Gabhann, O. Winqvist, B. Sundelin, C. Jefferies, B. Rozell, V. Kuchroo, and M. Wahren-Herlenius. 2009. Loss of the lupus autoantigen Ro52/Trim21 induces tissue inflammation and systemic autoimmunity by disregulating the IL-23-Th17 pathway. *J Exp Med* 206: 1661-1671.

116. Lombardi, V., L. Van Overtvelt, S. Horiot, and P. Moingeon. 2009. Human dendritic cells stimulated via TLR7 and/or TLR8 induce the sequential production of Il-10, IFN-gamma, and IL-17A by naive CD4+ T cells. *J Immunol* 182: 3372-3379.

117. Yu, C., W. Peng, J. Oldenburg, J. Hoch, T. Bieber, A. Limmer, G. Hartmann, W. Barchet, A. Eis-Hübinger, and N. Novak. 2010. Human plasmacytoid dendritic cells support Th17 cell effector function in response to TLR7 ligation. *J Immunol* 184: 1159-1167.

118. Vollmer, J., S. Tluk, C. Schmitz, S. Hamm, M. Jurk, A. Forsbach, S. Akira, K. Kelly, W. Reeves, S. Bauer, and A. Krieg. 2005. Immune stimulation mediated by autoantigen binding sites within small nuclear RNAs involves Toll-like receptors 7 and 8. *J Exp Med* 202: 1575-1585.

119. Morel, L. 2010. Genetics of SLE: evidence from mouse models. *Nat Rev Rheumatol* 6: 348-357.

120. Sobel, E., C. Mohan, L. Morel, J. Schiffenbauer, and E. Wakeland. 1999. Genetic dissection of SLE pathogenesis: adoptive transfer of Sle1 mediates the loss of tolerance by bone marrow-derived B cells. *J Immunol* 162: 2415-2421.

121. Sobel, E., M. Satoh, Y. Chen, E. Wakeland, and L. Morel. 2002. The major murine systemic lupus erythematosus susceptibility locus Sle1 results in abnormal functions of both B and T cells. *J Immunol* 169: 2694-2700.

122. Cuda, C. M., L. Zeumer, E. S. Sobel, B. P. Croker, and L. Morel. 2010. Murine lupus susceptibility locus Sle1a requires the expression of two sub-loci to induce inflammatory T cells. *Genes Immun* 11: 542-553.

123. Wu, H., S. A. Boackle, P. Hanvivadhanakul, D. Ulgiati, J. M. Grossman, Y. Lee, N. Shen, L. J. Abraham, T. R. Mercer, E. Park, L. A. Hebert, B. H. Rovin, D. J. Birmingham, D. M. Chang, C. J. Chen, D. McCurdy, H. M. Badsha, B. Y. H. Thong, H. H. Chng, F. C. Arnett, D. J. Wallace, C. Y. Yu, B. H. Hahn, R. M. Cantor, and B. P. Tsao. 2007. Association of a common complement receptor 2 haplotype with increased risk of systemic lupus erythematosus. *Proc Natl Acad Sci U S A* 104: 3961-3966.

124. Douglas, K., D. Windels, J. Zhao, A. Gadeliya, H. Wu, K. Kaufman, J. Harley, J. Merrill, R. Kimberly, G. Alarcón, E. Brown, J. Edberg, R. Ramsey-Goldman, M. Petri, J. Reveille, L. Vilá, P. Gaffney, J. James, K. Moser, M. Alarcón-Riquelme, T. Vyse, G. Gilkeson, C. Jacob, J. Ziegler, C. Langefeld, D. Ulgiati, B. Tsao, and S. Boackle. 2009. Complement receptor 2 polymorphisms associated with systemic lupus erythematosus modulate alternative splicing. *Genes Immun* 10: 457-469.

125. La Cava, A. 2009. Lupus and T cells. *Lupus* 18: 196-201.

126. Crispín, J. C., V. C. Kyttaris, C. Terhorst, and G. C. Tsokos. 2010. T cells as therapeutic targets in SLE. *Nat Rev Rheumatol* 6: 317-325.

127. Barnden, M. J., J. Allison, W. R. Heath, and F. R. Carbone. 1998. Defective TCR expression in transgenic mice constructed using cDNA-based alpha- and beta-chain genes under the control of heterologous regulatory elements. *Immunol Cell Biol* 76: 34-40.

128. Bettelli, E., Y. Carrier, W. Gao, T. Korn, T. B. Strom, M. Oukka, H. L. Weiner, and V. K. Kuchroo. 2006. Reciprocal developmental pathways for the generation of pathogenic effector TH17 and regulatory T cells. *Nature* 441: 235-238.

129. Rozen, S., and H. Skaletsky. 2000. Primer3 on the WWW for general users and for biologist programmers. *Methods Mol Biol* 132: 365-386.

130. Rocke, D. M., and B. Durbin. 2001. A model for measurement error for gene expression arrays. *J Comput Biol* 8: 557-569.

131. Dozmorov, I., and M. Centola. 2003. An associative analysis of gene expression array data. *Bioinformatics* 19: 204-211.

132. Morris, S. C., P. L. Cohen, and R. A. Eisenberg. 1990. Experimental induction of systemic lupus erythematosus by recognition of foreign Ia. *Clin Immunol Immunopathol* 57(2): 263-273.

133. Slavin, A., C. Ewing, J. Liu, M. Ichikawa, J. Slavin, and C. C. Bernard. 1998. Induction of a multiple sclerosis-like disease in mice with an immunodominant epitope of myelin oligodendrocyte glycoprotein. *Autoimmunity* 28: 109-120.

134. Josefowicz, S. Z., and A. Rudensky. 2009. Control of regulatory T cell lineage commitment and maintenance. *Immunity* 30: 616-625.

135. Stockinger, B., K. Hirota, J. Duarte, and M. Veldhoen. 2011. External influences on the immune system via activation of the aryl hydrocarbon receptor. *Semin Immunol* 23: 99-105.

136. Chen, Y., C. Cuda, and L. Morel. 2005. Genetic Determination of T Cell Help in Loss of Tolerance to Nuclear Antigens. *J Immunol* 174: 7692-7702.

137. Korn, T., M. Mitsdoerffer, and V. K. Kuchroo. 2010. Immunological basis for the development of tissue inflammation and organ-specific autoimmunity in animal models of multiple sclerosis. *Results Probl Cell Differ* 51: 43-74.

138. Giguère, V. 1999. Orphan nuclear receptors: from gene to function. *Endocr Rev* 20: 689-725.

139. Marinescu, V. D., I. S. Kohane, and A. Riva. 2005. MAPPER: a search engine for the computational identification of putative transcription factor binding sites in multiple genomes. *BMC Bioinformatics* 6: 79.

140. Ishii, H., and Y. Sakuma. 2011. Complex organization of the 5'-untranslated region of the mouse estrogen receptor α gene: Identification of numerous mRNA transcripts with distinct 5'-ends. *J Steroid Biochem Mol Biol* 125: 211-218.

141. Alaynick, W. A., J. M. Way, S. A. Wilson, W. G. Benson, L. Pei, M. Downes, R. Yu, J. W. Jonker, J. A. Holt, D. K. Rajpal, H. Li, J. Stuart, R. McPherson, K. S. Remlinger, C. Y. Chang, D. P. McDonnell, R. M. Evans, and A. N. Billin. 2010. ERRgamma regulates cardiac, gastric, and renal potassium homeostasis. *Mol Endocrinol* 24: 299-309.

142. Friese, A., J. A. Kaltschmidt, D. R. Ladle, M. Sigrist, T. M. Jessell, and S. Arber. 2009. Gamma and alpha motor neurons distinguished by expression of transcription factor Err3. *Proc Natl Acad Sci U S A* 106: 13588-13593.

143. Lorke, D. E., U. Süsens, U. Borgmeyer, and I. Hermans-Borgmeyer. 2000. Differential expression of the estrogen receptor-related receptor gamma in the mouse brain. *Brain Res Mol Brain Res* 77: 277-280.

144. Bookout, A. L., Y. Jeong, M. Downes, R. T. Yu, R. M. Evans, and D. J. Mangelsdorf. 2006. Anatomical profiling of nuclear receptor expression reveals a hierarchical transcriptional network. *Cell* 126: 789-799.

145. Alaynick, W. A., R. P. Kondo, W. Xie, W. He, C. R. Dufour, M. Downes, J. W. Jonker, W. Giles, R. K. Naviaux, V. Giguère, and R. M. Evans. 2007. ERRgamma directs and maintains the transition to oxidative metabolism in the postnatal heart. *Cell Metab* 6: 13-24.

146. Dufour, C. R., B. J. Wilson, J. M. Huss, D. P. Kelly, W. A. Alaynick, M. Downes, R. M. Evans, M. Blanchette, and V. Giguère. 2007. Genome-wide orchestration of cardiac functions by the orphan nuclear receptors ERRalpha and gamma. *Cell Metab* 5: 345-356.

147. Via, C. S. 2010. Advances in lupus stemming from the parent-into-F1 model. *Trends Immunol* 31: 236-245.

148. Choudhury, A., P. L. Cohen, and R. A. Eisenberg. 2010. B cells require "nurturing" by CD4 T cells during development in order to respond in chronic graft-versus-host model of systemic lupus erythematosus. *Clin Immunol* 136: 105-115.

149. Morel, L., Y. Yu, K. R. Blenman, R. A. Caldwell, and E. K. Wakeland. 1996. Production of congenic mouse strains carrying genomic intervals containing SLE-susceptibility genes derived from the SLE-prone NZM2410 strain. *Mamm Genome* 7: 335-339.

150. Steward-Tharp, S. M., Y. J. Song, R. M. Siegel, and J. J. O'Shea. 2010. New insights into T cell biology and T cell-directed therapy for autoimmunity, inflammation, and immunosuppression. *Ann N Y Acad Sci* 1183: 123-148.

151. Glass, C. K., and K. Saijo. 2010. Nuclear receptor transrepression pathways that regulate inflammation in macrophages and T cells. *Nat Rev Immunol* 10: 365-376.

152. Pernis, A. B. 2007. Estrogen and CD4+ T cells. *Curr Opin Rheumatol* 19: 414-420.

153. Mora, J. R., M. Iwata, and U. H. von Andrian. 2008. Vitamin effects on the immune system: vitamins A and D take centre stage. *Nat Rev Immunol* 8: 685-698.

154. Giguère, V. 2008. Transcriptional control of energy homeostasis by the estrogen-related receptors. *Endocr Rev* 29: 677-696.

155. Eichner, L. J., and V. Giguère. 2011. Estrogen related receptors (ERRs): A new dawn in transcriptional control of mitochondrial gene networks. *Mitochondrion* 11: 544-552.

156. Takayanagi, S., T. Tokunaga, X. Liu, H. Okada, A. Matsushima, and Y. Shimohigashi. 2006. Endocrine disruptor bisphenol A strongly binds to human estrogen-related receptor gamma (ERRgamma) with high constitutive activity. *Toxicol Lett* 167: 95-105.

157. Michalek, R. D., and J. C. Rathmell. 2010. The metabolic life and times of a T-cell. *Immunol Rev* 236: 190-202.

158. Vander Heiden, M. G., L. C. Cantley, and C. B. Thompson. 2009. Understanding the Warburg effect: the metabolic requirements of cell proliferation. *Science* 324: 1029-1033.

159. Jacobs, S. R., C. E. Herman, N. J. Maciver, J. A. Wofford, H. L. Wieman, J. J. Hammen, and J. C. Rathmell. 2008. Glucose uptake is limiting in T cell activation and requires CD28-mediated Akt-dependent and independent pathways. *J Immunol* 180: 4476-4486.

160. Michalek, R. D., V. A. Gerriets, S. R. Jacobs, A. N. Macintyre, N. J. MacIver, E. F. Mason, S. A. Sullivan, A. G. Nichols, and J. C. Rathmell. 2011. Cutting edge: distinct glycolytic and lipid oxidative metabolic programs are essential for effector and regulatory CD4+ T cell subsets. *J Immunol* 186: 3299-3303.

161. Liu, D., Z. Zhang, and C. T. Teng. 2005. Estrogen-related receptor-gamma and peroxisome proliferator-activated receptor-gamma coactivator-1alpha regulate estrogen-related receptor-alpha gene expression via a conserved multi-hormone response element. *J Mol Endocrinol* 34: 473-487.

162. Wang, L., J. Liu, P. Saha, J. Huang, L. Chan, B. Spiegelman, and D. D. Moore. 2005. The orphan nuclear receptor SHP regulates PGC-1alpha expression and energy production in brown adipocytes. *Cell Metab* 2: 227-238.

163. Giguère, V. 2002. To ERR in the estrogen pathway. *Trends Endocrinol Metab* 13: 220-225.

164. Hong, H., L. Yang, and M. R. Stallcup. 1999. Hormone-independent transcriptional activation and coactivator binding by novel orphan nuclear receptor ERR3. *J Biol Chem* 274: 22618-22626.

165. Huppunen, J., G. Wohlfahrt, and P. Aarnisalo. 2004. Requirements for transcriptional regulation by the orphan nuclear receptor ERRgamma. *Mol Cell Endocrinol* 219: 151-160.

166. Castet, A., A. Herledan, S. Bonnet, S. Jalaguier, J. M. Vanacker, and V. Cavaillès. 2006. Receptor-interacting protein 140 differentially regulates estrogen receptor-related receptor transactivation depending on target genes. *Mol Endocrinol* 20: 1035-1047.

167. Chao, E. Y., J. L. Collins, S. Gaillard, A. B. Miller, L. Wang, L. A. Orband-Miller, R. T. Nolte, D. P. McDonnell, T. M. Willson, and W. J. Zuercher. 2006. Structure-guided synthesis of tamoxifen analogs with improved selectivity for the orphan ERRgamma. *Bioorg Med Chem Lett* 16: 821-824.

168. Coward, P., D. Lee, M. V. Hull, and J. M. Lehmann. 2001. 4-Hydroxytamoxifen binds to and deactivates the estrogen-related receptor gamma. *Proc Natl Acad Sci U S A* 98: 8880-8884.

169. Plutzky, J. 2011. The PPAR-RXR transcriptional complex in the vasculature: energy in the balance. *Circ Res* 108: 1002-1016.

BIOGRAPHICAL SKETCH

Daniel was born and raised in Rhode Island where he graduated from Toll Gate High School with honors in 1994. His affinity to nature, biology, and physiology led him to pursue pre-veterinary medicine at the University of Vermont where he earned his B.S. in Animal Sciences in 1998. While there, he also gained valuable laboratory experience in a work-study program under the guidance of Dr. Karen Plaut and Dr. Woody Panky, and was even given his own project in a dairy milk research lab. After graduation, he spent time back in Rhode Island as a veterinary technician, but it was his undergraduate research experience that led him to pursue a laboratory manager position for Dr. Laurence Morel when he moved to Gainesville. The challenges and excitement of scientific discovery eventually swayed him to forgo veterinary medicine and to enroll in the graduate program in the University of Florida's College of Medicine. A special interest in immunology and autoimmunity led him to return to Dr. Morel's lab in the spring of 2006 where he was offered a position as a graduate research assistant studying a congenic model of murine lupus.